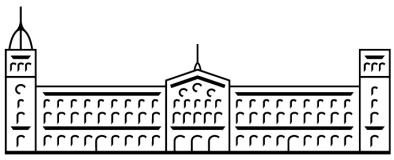

**Treball final de grau**

**GRAU DE MATEMÀTIQUES**

**Facultat de Matemàtiques i Informàtica**
**Universitat de Barcelona**

# Introduction to computational fluid dynamics

**Autor: Ricard Monge Calvo**

**Director:** **Dr. Angel Jorba**
**Realitzat a:** **Departament de Matemàtiques i Informàtica (UB)**
**Centre Tecnològic de Transferència de Calor (UPC)**

**Barcelona,** **18 de gener de 2018**

# Contents

# Introduction

The study of fluid dynamics has been a very important subject since ancient times. From the civil engineering applications in roman empire until the study of the air flow in aeronautical engineering, many significant physical applications of fluid dynamics problems are present in human history. However, in the present day with the use of applied mathematics and the power of computation, the focus of fluid dynamics has changed from practical physical experiments to computational simulations. For this reason, it is important to have a solid and rigorous mathematical framework in which to develop the computational solutions of this simulations.

The purpose of this study is to give an introduction to computational dynamics by establishing a mathematical framework for the fluid's particles and properties and explaining computational methods in this framework to compute the flow of a fluid in certain conditions (incompressibility and homogeneity). We will divide this study in three parts.

The first part contains the mathematical definition of a fluid and it's properties. We define a fluid, it's flow and it's properties and derive the differential equations that give the evolution of the fluid flow, the Navier-Stokes equations, and the evolution of general properties. Furthermore, we define the incompressible and homogeneous conditions for a fluid and derive consequences of this conditions.

In the second part, we give the discretization of the differential equations that give the evolution of the fluid's properties. In particular, we present two types of spatial discretizations and present a scheme for temporal discretizations. In addition, we give an example of discretization using the methods described. Finally, we explain a way to compute the numerical solution of the discretized equations.

In the third chapter we give two examples of fluid dynamics problems that we solve computationally using the previously explained mathematical framework and discretization methods. The first example is a two dimensional flow where we compute how a scalar property transports through the fluid with time. The second example is a two dimensional fluid, initially at rest, where the upper boundary is moving with uniform velocity, where we study the evolution of the velocity field of the fluid with time until a stationary state.

This study was done in collaboration with the *Centre Tecnològic de Transferència de Calor* (UPC), with the help of Arnau Pont and under the supervision of Dr. Asensi Oliva.

# Chapter 1

# Mathematical model of a fluid

## 1.1 Definition of a fluid

The first step to study the flow of a fluid is to properly settle how to define a fluid and its properties.
However, in order to define these we need to make the continuum assumption, describing the fluid as a continuous body (made of infinite point particles) without taking into account its molecular structure. For most macroscopic applications and phenomena this is an accurate description.

**Definition 1.1.** Let $\Omega$ be a domain, that is a connected open subset of a vector space, in $\mathbb{R}^n$ (for $n \in \{2,3\}$) vector space over the field $\mathbb{R}$; such that $\Omega$ is compact and has a smooth boundary $\partial\Omega$. A fluid is then defined as a subdomain $\Omega_0 \subseteq \Omega$.

Intuitively, the subdomain represents the space occupied by the fluid and the points inside the subdomain are the particles of the fluid. In most common applications we will have $\Omega_0 = \Omega$ (that is the fluid occupies the whole space where it is contained).

**Definition 1.2.** Given a fluid $\Omega_0 \subseteq \Omega$ we define its flow map in a given time interval $[0,T]$ for $T \in \mathbb{R}$ as the application:

$$\zeta : \Omega_0 \times [0,T] \longrightarrow \Omega$$

where $\zeta(\vec{x},t) = \vec{x}(t)$ gives the new position of the fluid particle and $\zeta(\Omega_0,t) = \Omega_t \subseteq \Omega \ \forall t \in [0,T]$ is the subdomain of the fluid at any given time. We impose that this subdomain is also compact and has a smooth boundary $\partial\Omega_t \ \ \forall t \in [0,T]$. As stated above, in most common applications we will have $\Omega_t = \Omega \ \forall t \in [0,T]$.

**Definition 1.3.** We define the properties of the fluid flow in a given time interval $[0,T]$ for $T \in \mathbb{R}$ as the following applications:

- $\vec{u} : \Omega \times [0,T] \longrightarrow \mathbb{R}^n$ called the velocity field of the fluid (vector field). This property shows how the particles that make the fluid move through time.
- p: $\Omega \times [0,T] \longrightarrow \mathbb{R}$ called the pressure field of the fluid (scalar field). This property measures the force balance applied on a certain surface of the fluid, and on the surfaces of smaller regions inside it.
- $\rho : \Omega \times [0,T] \longrightarrow \mathbb{R}$ called the density field, or mass density field, of the fluid (scalar field). This property describes the amount of particles in a certain volume of the fluid's subdomain.

These properties will characterize how the fluid evolves through time, as we will see in the following sections.

**Comment 1.**Given that the flow of a specific particle of the fluid is given by $\vec{x}_0(t) = \zeta(\vec{x}_0, t)$ we see that its velocity is $\frac{\partial \vec{x}_o}{\partial t} = \frac{\partial \zeta(\vec{x}_0,t)}{\partial t}$. Therefore, the velocity field of the fluid is specified as:

$$\vec{u}(\vec{x},t) = \frac{\partial \zeta(\vec{x},t)}{\partial t} = \frac{\partial \vec{x}(t)}{\partial t} \quad \forall \vec{x} \in \Omega_t \; and \; \forall t \in [0,T].$$

By being able to calculate the velocity field of the fluid we will be able to specify the fluid flow application $\zeta(\vec{x}_0, t)$.

**Comment 2.** Although the properties are defined in the whole domain $\Omega$ as a technical requisite (as all $\Omega_t \subseteq \Omega$) it is trivially assumed that the values of the properties outside the fluid's subdomain in a given time are 0.

**Comment 3.** The property applications defined above are assumed to be sufficiently smooth and well behaved, so that the functions are differentiable (actually $C^\infty$). We can define them like this because of the initial continuum assumption.

## 1.2 Fluid flow. Navier-Stokes equations

Now that we have defined the properties that characterize the fluid's flow, we take a look on how the flow changes over time, and that is given by the property $\vec{u}$. The behavior of $\vec{u}$ is given by the following differential equations, called the Navier-Stokes equations (in its most general formulation):

$$\frac{\partial}{\partial t}(\rho\vec{u}) + (\vec{u}\cdot\vec{\nabla})(\rho\vec{u}) + (\rho\vec{u})\vec{\nabla}\cdot\vec{u} = \rho\vec{g} + \vec{\nabla}\sigma \tag{1.1}$$

$$\frac{\partial}{\partial t}\rho + \vec{\nabla}(\rho\vec{u}) = 0 \tag{1.2}$$

where $\vec{\nabla}$ is the nabla differential operator (in Cartesian coordinates $\vec{\nabla} = (\frac{\partial}{\partial x}, \frac{\partial}{\partial y}, \frac{\partial}{\partial z})$); $\vec{g}(\vec{x}, t) \in \mathbb{R}^n$ is the body forces vector, that represents the external body forces applied to the fluid (e.g. gravity, magnetic force, etc); and $\sigma$ is the stress tensor, which represents the surface forces acting on the fluid (e.g. frictional forces, viscosity, etc).

Equation (1.1) is called Momentum equation and equation (1.2) is called Mass equation. These names will make sense in the derivation of the equations, as they are derived from the conservation of these magnitudes.

### 1.2.1 Derivation of the Navier-Stokes equations

In the following section, we are going to derive the Navier-Stokes equations using the following physical conservation principles: mass conservation and momentum conservation.

Nonetheless, in order to derive the equations we will need some previous results.

Given a scalar property of a fluid $\phi(\vec{x}, t)$, using Cartesian coordinates we have:

$$\frac{d}{dt}\phi(\vec{x}, t) = \frac{\partial\phi}{\partial t} + \sum_{i=1}^{3} \frac{\partial\phi}{\partial x_i}\frac{\partial x_i}{\partial t} = \frac{\partial\phi}{\partial t} + \vec{u}\cdot\vec{\nabla}\phi$$

**Definition 1.4.** We define a material derivative as the linear differential operator:

$$\frac{D}{Dt} = \frac{\partial}{\partial t} + \vec{u}\cdot\vec{\nabla}$$

which shows the variation of the derivated property following the movement of the fluid particles. As we have seen, all the time derivatives of the properties in a fluid can be regarderd as material derivatives.

**Theorem 1.5** (Divergence theorem)**.** Let $A$ be a subset of $\mathbb{R}^n$ that is compact and has a piecewise smooth boundary $\partial A$ and let $\vec{f}$ be a vector field defined in a neighborhood of $A$ that is $C^1$ (continuously differentiable), then the following equality holds:

$$\int_A (\vec{\nabla}\cdot\vec{f})\, dV = \int_{\partial A} (\vec{f}\cdot\vec{n})\, dS. \tag{1.3}$$

**Theorem 1.6** (Reynolds transport theorem)**.** Let $\Sigma_t$ be an arbitrary open region of a fluid $\forall t \in [0, T]$ and let $\phi(\vec{x}, t)$ be a scalar function or property associated with the fluid. Then it holds that:

$$\frac{d}{dt}\left[\int_{\Sigma_t} \phi(\vec{x}, t) d\vec{x}\right] = \int_{\Sigma_t} \left[\frac{\partial}{\partial t}\phi + \vec{\nabla}(\phi\vec{u}) d\vec{x}\right] \quad \forall t \in [0, T]. \tag{1.4}$$

Let's look at the proof of this last transport theorem.

*Proof.* We recall that the fluid flow map $\zeta(\vec{x}, t) = \vec{x}(t)$ gives us the change of position of a fluid particle and that any region (made up of fluid particles) $\Sigma_0$ changes to another region $\Sigma_t$ from time $t_0 = 0$ to a given $t \in [0, T]$. Then, given a fluid property $\phi(\vec{x}, t)$ we have:

$$\int_{\Sigma_t} \phi(\vec{x}, t) d\vec{x} = \int_{\Sigma_0} \phi(\zeta(\vec{x}, t), t) J(\vec{x}, t) d\vec{x}$$

where we have used a change of variables from $\vec{x}$ to $\zeta(\vec{x}, t)$ such that $J(\vec{x}, t)$ is the determinant of the Jacobian matrix of the map $\zeta(\vec{x}, t)$ for a given $t \in [0, T]$. With this change of variables, as $\Sigma_0$ is a constant region of $\Omega$, we can derivate under the integration sign and get:

$$\frac{d}{dt}\int_{\Sigma_t} \phi(\vec{x}, t) d\vec{x} = \frac{d}{dt}\int_{\Sigma_0} \phi(\zeta(\vec{x}, t), t) J(\vec{x}, t) d\vec{x} = \int_{\Sigma_0} \frac{d}{dt}\left[\phi(\zeta(\vec{x}, t), t) J(\vec{x}, t)\right] d\vec{x}.$$

Now we have to look at the derivative of the expression $\phi(\zeta(\vec{x}, t), t) J(\vec{x}, t)$. As we stated above, the time derivative of a scalar property of the fluid is equal to the material derivative, and such we have:

$$\frac{d}{dt}\left(\phi(\zeta(\vec{x}, t), t) J(\vec{x}, t)\right) = \left(\frac{D}{Dt}\phi(\zeta(\vec{x}, t), t)\right) J(\vec{x}, t) + \phi(\zeta(\vec{x}, t), t)\frac{d}{dt} J(\vec{x}, t).$$

For the term $\frac{d}{dt} J(\vec{x}, t)$ we will use the following lemma:

**Lemma 1.7.**

$$\frac{d}{dt} J(\vec{x}, t) = J(\vec{x}, t)(\vec{\nabla} \cdot \vec{u}(\zeta(\vec{x}, t), t))$$

which can be easily proved by direct calculation of the partial derivatives.

Substituting these results in the previous expression for the time derivative of the integral of the property $\phi(\vec{x}, t)$ we get:

$$\frac{d}{dt}\int_{\Sigma_t} \phi(\vec{x}, t) d\vec{x} = \ldots = \int_{\Sigma_0} \left[\left(\frac{D}{Dt}\phi(\zeta(\vec{x}, t), t)\right) + \phi(\vec{\nabla} \cdot \vec{u})(\zeta(\vec{x}, t), t)\right] J(\vec{x}, t)\, d\vec{x}.$$

If we change back the variables from $\zeta(\vec{x}, t)$ to $\vec{x}$ we get:

$$\frac{d}{dt}\int_{\Sigma_t} \phi(\vec{x}, t) d\vec{x} = \int_{\Sigma_t} \left[\left(\frac{D}{Dt}\phi(\vec{x}, t)\right) + \phi(\vec{\nabla} \cdot \vec{u})(\vec{x}, t)\right] d\vec{x} = \int_{\Sigma_t} \left[\frac{\partial}{\partial t}\phi + \vec{\nabla}(\phi\vec{u})\right] d\vec{x}$$

which ends our proof. □

### Conservation of Mass

Given that the mass of an open region of the fluid $\Sigma_t$ $\forall t \in [0, T]$ is given by the integration of its density over the region, and this mass is conserved $\forall t \in [0, T]$, we have:

$$M_\Sigma := \int_{\Sigma_0} \rho(\vec{x}, 0) d\vec{x} = \int_{\Sigma_t} \rho(\vec{x}, t) d\vec{x} \ \ \forall t \in [0, T].$$

The conservation of the mass of the fluid implies the following, using the transport theorem:

$$\frac{dM_\Sigma}{dt} = 0 \to 0 = \int_{\Sigma_t} \left[ \frac{\partial}{\partial t} \rho + \vec{\nabla}(\rho \vec{u}) \right] d\vec{x} \ \ \forall t \in [0, T]$$

and this is valid for any region $\Sigma_t$ of the initial fluid, that is for any arbitrary small region inside $\Omega_t$. Therefore, the integrand must vanish, so:

$$\frac{\partial}{\partial t} \rho + \vec{\nabla}(\rho \vec{u}) = 0$$

that gives the Mass equation (1.2). Using the material derivative, we can get another form for the Mass equation:

$$\frac{D}{Dt} \rho + \rho(\vec{\nabla} \cdot \vec{u}) = 0$$

### Conservation of Momentum

Given that the momentum of an open region of the fluid $\Sigma_t$ $\forall t \in [0, T]$ is given by:

$$\vec{m}(t) = \int_{\Sigma_t} \rho(\vec{x}, t) \vec{u}(\vec{x}, t) d\vec{x} \ \ \forall t \in [0, T].$$

By Newton's second law and using the transport theorem (component-wise for the velocity field) we have that:

$$\sum (\textit{Forces acting on the region}) = \frac{d\vec{m}(t)}{dt} = \int_{\Sigma_t} \left[ \frac{\partial(\rho \vec{u})}{\partial t} + \vec{\nabla}((\rho \vec{u}) \vec{u}) \right] d\vec{x} =$$

$$= \int_{\Sigma_t} \left[ \frac{\partial(\rho \vec{u})}{\partial t} + (\vec{u} \cdot \vec{\nabla})(\rho \vec{u}) + (\rho \vec{u})(\vec{\nabla} \cdot \vec{u}) \right] d\vec{x} \ \ \forall t \in [0, T].$$

Now we have to calculate the term involving the forces. We can distinguish between two different forces affecting the fluid: external body forces that exert a force over a volume, represented by the body force density $\vec{g}(\vec{x}, t)$; and stress forces that exert a force over the surface of a volume, represented by the stress

tensor $\sigma(\vec{x}, t)$. We have the following expression for the forces affecting a region $\Sigma_t$:

$$\sum(\textit{Forces acting on the region } \Sigma_t) = \int_{\Sigma_t} \rho\vec{g}\, d\vec{x} + \int_{\partial\Sigma_t} \sigma \cdot \vec{n}\, dS.$$

Note that the stress forces are integrated over the surface of the volume, where they act, and using the surface differential $dS$. Moreover, as the tensor need not be parallel to the surface of the volume we need to project it by calculating the dot product with $\vec{n}$.

Finally we can use the divergence theorem in the term with the surface forces and get the following expression:

$$\int_{\Sigma_t} \left[\rho\vec{g} + \vec{\nabla}\sigma\right]\, d\vec{x} = \int_{\Sigma_t} \left[\frac{\partial(\rho\vec{u})}{\partial t} + (\vec{u}\cdot\vec{\nabla})(\rho\vec{u}) + (\rho\vec{u})(\vec{\nabla}\cdot\vec{u})\right] d\vec{x} \;\; \forall t \in [0, T].$$

As our arguments were done for an arbitrary small region of $\Omega_t$ $\forall t \in [0, T]$, the equality holds for the integrands alone:

$$\rho\vec{g} + \vec{\nabla}\sigma = \frac{\partial(\rho\vec{u})}{\partial t} + (\vec{u}\cdot\vec{\nabla})(\rho\vec{u}) + (\rho\vec{u})(\vec{\nabla}\cdot\vec{u}) \tag{1.5}$$

that gives the Momentum equation (1.1).

### 1.2.2 Incompressible fluids

One of the most studied fluids are the incompressible fluids, as most liquids are regarded as quasi-incompressible in most practical aplications. Let's look at the exact definition of an incompressible fluid:

**Definition 1.8.** Given a fluid $\Omega_t$ $\forall t \in [0, T]$ we say it is incompressible if for any region inside the fluid $\Sigma_t$ it holds that:

$$\textit{Volume}(\Sigma_t) = \int_{\Sigma_t} d\vec{x} = \textit{constant} \iff \frac{d}{dt}\int_{\Sigma_t} d\vec{x} = 0 \;\; \forall t \in [0, T].$$

Let see what this means with the following proposition.

**Proposition 1.9.** Given a fluid $\Omega_t$ $\forall t \in [0, T]$ with flow map $\zeta(\vec{x}, t)$ such that $\vec{u} = \frac{\partial\zeta(\vec{x},t)}{\partial t}$ and $J$ is the jacobian of $\zeta(\vec{x}, t)$, the following statements are equivalent:

1. The fluid is incompressible;
2. $\vec{\nabla}\cdot\vec{u} = 0$;
3. $J \equiv 1$.

*Proof.* During the proof of the transport theorem we used a change of variables to change the integration domain $\Sigma_t$ into the initial $\Sigma_0$ which is a constant region. In this case, when we apply this change of variables to the definition of incompressible fluid we get:

$$0 = \frac{d}{dt}\int_{\Sigma_t} d\vec{x} = \frac{d}{dt}\int_{\Sigma_0} J(\vec{x},t)d\vec{x} = \int_{\Sigma_0}(\vec{\nabla}\cdot\vec{u})Jd\vec{x} = \int_{\Sigma_t}(\vec{\nabla}\cdot\vec{u})d\vec{x}$$

which implies statements 2. and 3. if, and only if, statement 1. is true. □

From the previous proposition, we get that for incompressible fluids the Navier-Stokes equations end up in the following form:

$$\frac{\partial}{\partial t}(\rho\vec{u}) + (\vec{u}\cdot\vec{\nabla})(\rho\vec{u}) = \rho\vec{g} + \vec{\nabla}\sigma \tag{1.6}$$

$$\frac{\partial}{\partial t}\rho + (\vec{u}\cdot\vec{\nabla})\rho = \frac{D}{Dt}\rho = \frac{d}{dt}\rho = 0 \tag{1.7}$$

However, from equation (1.7) we can get further inside to the incompressibility condition. The condition $\frac{D}{Dt}\rho = 0$ means that the density of the studied fluid is constant while following the fluid. From a more physical point of view, if we take a region of fluid $\Sigma_0$ this region's overall density will remain the same even if the shape of the region, and its position, changes with the movement of the fluid (thus also maintaining the volume of the region) as if the region was not being disturbed by the surrounding fluid, only moved by it.

Aside from incompressible fluids, we can define another type of fluid, homogeneous fluids:

**Definition 1.10.** Given a fluid $\Omega_t$ $\forall t \in [0,T]$ we say it's homogeneous if $\rho(\vec{x},t) = \rho(t)$ $\forall\vec{x}\in\Omega_t$ given a $t\in[0,T]$, that is the density of the fluid is constant in space.

To conclude, we can see that joining the definitions of incompressible and homogeneous fluids we get that $\rho(\vec{x},t) = \rho_\infty = constant$ $\forall\vec{x}\in\Omega_t$ $\forall t\in[0,T]$.

In our study of numerical solutions to the Navier-Stokes equations we will only consider incompressible homogeneous fluids (thus having $\rho(\vec{x},t) = \rho_\infty$). For incompressible homogeneous fluids, the Navier-Stokes equations end up as:

$$\frac{\partial}{\partial t}\vec{u} + (\vec{u}\cdot\vec{\nabla})\vec{u} = \vec{g} + \frac{1}{\rho_\infty}\vec{\nabla}\sigma \tag{1.8}$$

$$\vec{\nabla}\cdot\vec{u} = 0 \tag{1.9}$$

### 1.2.3 The stress tensor

As seen in previous sections, the behavior of the velocity field of the fluid $\vec{u}$ heavily depends on the forces applied to the fluid, the external body forces and the surface forces given by the stress tensor. Setting the body forces aside, it is then important which stress tensor we use for our Momentum equation. In our study, we consider two different models for the stress tensor:

- Stress tensor for inviscid fluids, where we neglect the internal friction between the particles of the fluid, then the stress tensor can be modeled as:

$$\sigma(\vec{x},t) := -p(\vec{x},t)\mathbb{I} = -p(\vec{x},t)\begin{pmatrix} 1 & 0 & 0 \\ 0 & 1 & 0 \\ 0 & 0 & 1 \end{pmatrix}$$

  then the momentum equation ends up as:

$$\frac{\partial}{\partial t}(\rho\vec{u}) + (\vec{u}\cdot\vec{\nabla})(\rho\vec{u}) + (\rho\vec{u})\vec{\nabla}\cdot\vec{u} + \vec{\nabla}p = \rho\vec{g}. \tag{1.10}$$

  In our case for incompressible homogeneous fluids we end up with the equation:

$$\frac{\partial}{\partial t}\vec{u} + (\vec{u}\cdot\vec{\nabla})\vec{u} + \frac{1}{\rho_\infty}\vec{\nabla}p = \vec{g}. \tag{1.11}$$

- Stress tensor for viscous fluids, where we incorporate a model for the internal friction of the fluid particles, which leads to the next stress tensor:

$$\sigma := -p\mathbb{I} + \tau.$$

  Now we have a viscous term, aside from the contribution of pressure, which can be modeled in the following way (for further reference on the viscous term see [1] and [3]):

$$\sigma := (-p + \lambda\vec{\nabla}\cdot\vec{u})\mathbb{I} + 2\mu\delta$$

  where $\lambda$ and $\mu$ are material constants; and $\delta := \frac{1}{2}[(\frac{\partial u_i}{\partial x_j} + \frac{\partial u_j}{\partial x_i})]_{i,j=1,2,3}$ is called the strain tensor, in Cartesian coordinates.

  This stress tensor leads to the following Momentum equation:

$$\frac{\partial}{\partial t}(\rho\vec{u}) + (\vec{u}\cdot\vec{\nabla})(\rho\vec{u}) + (\rho\vec{u})\vec{\nabla}\cdot\vec{u} + \vec{\nabla}p = (\lambda+\mu)\vec{\nabla}(\vec{\nabla}\cdot\vec{u}) + \mu\Delta\vec{u} + \rho\vec{g}. \tag{1.12}$$

In the case of incompressible homogeneous fluids, which will be the case of our study, we end up with the following Momentum equation:

$$\frac{\partial}{\partial t}\vec{u} + (\vec{u}\cdot\vec{\nabla})\vec{u} + \frac{1}{\rho_\infty}\vec{\nabla}p = \frac{\mu}{\rho_\infty}\Delta\vec{u} + \vec{g}. \tag{1.13}$$

**Definition 1.11.** We define the following constants: $\mu$ which is called dynamic viscosity and $\nu := \frac{\mu}{\rho_\infty}$ called kinematic viscosity.

Then the Momentum equations ends up as:

$$\frac{\partial}{\partial t}\vec{u} + (\vec{u}\cdot\vec{\nabla})\vec{u} + \frac{\nu}{\mu}\vec{\nabla}p = \nu\Delta\vec{u} + \vec{g}. \tag{1.14}$$

In our study we will only consider this two models for the stress tensor. That is, we will only consider inviscid fluids and viscous fluids.

**Comment 1.** It is clear from the Momentum equations given above (1.14) and (1.11) that the pressure $p$ is determined up to an additive constant, that is if p is a solution of a certain fluid flow problem, then $p' = p + C$ for $C \in \mathbb{R}$ is also a solution.

### 1.2.4 Initial conditions of the Navier-Stokes equations

Given the equations for an incompressible homogeneous viscous flow (1.13) and (1.7) are second order partial differential equations for $\vec{u}$ and first order partial differential equations for $p$, we have 4 equations and 4 variables (counting $\vec{u}$ component-wise). Therefore, we will need to assume some initial conditions in order to ensure the existence, uniqueness and smoothness of the solutions. Mainly, we need to specify initial values for the velocity field $\vec{u}(\vec{x}, 0)$, the pressure field $p(\vec{x}, 0)$ and the density $\rho(\vec{x}, 0) = \rho_\infty$ in addition to boundary conditions $\forall t \in [0, T]$.

We will not consider any external body forces in this section. If considered, the body force density vector $\vec{g}$ would have to be specified $\forall\vec{x} \in \Omega_t$ and $\forall t \in [0, T]$.

Regarding the boundary conditions, it is trivial to see that as the Mass equation has to hold for every region in the fluid's subdomain, the same equation has to hold in the whole subdomain, and therefore:

$$\int_{\Omega_t} \vec{\nabla}\cdot\vec{u}\, d\vec{x} = 0.$$

Furthermore, we mention an important distinction in the boundary conditions.

The ideal fluid conditions state that no fluid enters or leaves the subdomain and therefore, if $\vec{n}$ is the vector that represents the normal exterior direction of $\partial\Omega_t \ \ \forall t \in [0,T]$, we have $\vec{u}(\vec{x},t)\cdot\vec{n} = 0 \ \ \forall \vec{x} \in \partial\Omega_t$ and $\forall t \in [0,T]$. This conditions may also impose that the tangential velocity to the boundary $\vec{u}_t$ is also 0 (no-slip condition) or that we have no frictional losses $\partial\vec{u}_t/\partial\vec{n} = 0$ (free-slip condition).

On the other hand, we may have inflow conditions where $\vec{u}(\vec{x},t)\cdot\vec{n} \neq 0$ in some region of the boundary, but then the velocities at the boundary must be given $\forall t \in [0,T]$; and outflow conditions where the normal component of the velocity $\vec{u}_n$ and the tangential component $\vec{u}_t$ (normal and tangential to $\partial\Omega_t$) satisfy $\partial\vec{u}_n/\partial\vec{n} = 0$ *and* $\partial\vec{u}_t/\partial\vec{n} = 0$, that is the velocity does not change in the boundary and the fluid leaves the domain.

Finally, we may have the velocities in the boundary given $\forall t \in [0,T]$ by some arbitrary function. It obvious then than these velocities have to satisfy the Mass equation given above to be acceptable for the problem.

More generally, in the two dimensional fluid flow case, for incompressible homogeneous viscous (and inviscid) fluids it is known that given initial values for the velocity field $\vec{u}(\vec{x},0)$, the pressure field $p(\vec{x},0)$ and the density $\rho(\vec{x},0) = \rho_\infty$ in addition to boundary conditions $\forall t \in [0,T]$ a unique smooth solution exists, even when $T \to \infty$ (see [5]).

Regarding the three dimensional problem, it is known that unique smooth solutions for the problem exists only for a bounded time interval, where the maximum time of the interval, called blowup time, is determined by the initial velocities. The existence and uniqueness of the problem for $T \to \infty$ is and open problem (see [6] and [7]).

## 1.3 Dynamic similarities of fluid flows. Reynolds number

The study of macroscopic fluids is often associated with real problems regarding fluids in engineering and physical applications. For instance when talking about aerospace engineering, the study of the air flow around the wings of a plane is a common macroscopic fluid flow application. When we get a numerical solution for one such applications, it is then important to compare it to the real

case reference values, to ascertain the fidelity and accuracy of the model used.

However, in most cases in order to get this reference values one can not reproduce in full scale the application, or it is really expensive to do it. In this cases, a scale model of the problem is reproduced to obtain reference values, trying to get an equivalent fluid flow problem in a smaller scale. For this reason, it is important to study the scaling properties of the Navier-Stokes equations to define when two fluid flows of different parameters and scales can be regarded as similar.

Generally speaking, two fluid flows will have equivalent behavior when the fluid flow velocity field $\vec{u}$ evolves in the same way, that is their Navier-Stokes equations are equivalent, in spite of the dimensions of the properties involved. To specify what this means in a more technical way, we will develop a dimensionless form of the Navier-Stokes equations, then compare the dimensionless equations of the two fluid flows and see if they evolve in the same way.

In order to get a dimensionless variable, a common practice is to divide the variable by its characteristic value. This value is often arbitrary and depends on the problem considered. For instance, if we have a characteristic length $L$ and a characteristic velocity $U$ for our incompressible homogeneous viscous fluid, we can define dimensionless variables in the following way:

$$\vec{x}' := \frac{\vec{x}}{L}, \quad \vec{u}' := \frac{\vec{u}}{U}, \quad t' := \frac{t}{L/U} = \frac{Ut}{L}, \quad p' := \frac{p}{\rho_\infty U^2} \tag{1.15}$$

where we have used the fact that the dimensions of the pressure property are $[P] = \frac{Force}{Length^2} = \frac{Mass}{Length \cdot Time^2} = \frac{Mass}{Length^3} \cdot \frac{Length^2}{Time^2} = [\rho] \cdot [\vec{u}]^2$.

Then, we can derive the dimensionless form of the Momentum equation which ends up as:

$$\frac{\partial \vec{u'}}{\partial t'} + (\vec{u'} \cdot \vec{\nabla}')\vec{u'} + \frac{1}{\rho_\infty}\vec{\nabla}' p' = \frac{\mu}{\rho_\infty L U}\Delta' \vec{u'} + \frac{L}{U^2}\vec{g}$$

by changing the variables as well as the nabla operator. From this expression of the Momentum equations we can define two dimensionless numbers that will help us establish the dynamical similarities of flows.

**Definition 1.12.** For an incompressible homogeneous viscous fluid $\Omega_t \subseteq \Omega \ \forall t \in [0, T]$ such that we have a characteristic length $L$ and velocity $U$, we can define a variable change like (1.15) and the following two constants, characteristic to a concrete problem:

$$Re := \frac{\rho_\infty L U}{\mu} \quad and \quad Fr := \frac{U}{\sqrt{L\|\vec{g}\|}} \tag{1.16}$$

called respectively Reynolds and Froude numbers.

The latter constant helps us introduce a dimensionless body force vector $\vec{g'} := \frac{L}{U^2}\vec{g} = \frac{1}{Fr^2}\frac{\vec{g}}{\|\vec{g}\|}$. With these, we can reformulate the dimensionless Navier-Stokes equation as follows:

$$\frac{\partial \vec{u'}}{\partial t'} + (\vec{u'} \cdot \vec{\nabla'})\vec{u'} + \frac{1}{\rho_\infty}\vec{\nabla'}p' = \frac{1}{Re}\Delta'\vec{u'} + \vec{g'}. \tag{1.17}$$

Intuitively, the Reynolds number gives a relation between the fluid's inertial forces (given by the fluid's own movement) and its viscous forces that arise from friction of the fluid's particles. For low Reynolds numbers the viscous forces are more important, called high viscous fluid, whereas for high Reynolds numbers the inertial forces are more important. However, it is important to note that although for high Reynolds numbers inertial forces are more important, viscous forces can not be neglected as this forces are the origin of more complex phenomena, vorticity and turbulence.

On the other hand, the Froude number represents the relation between the inertial forces and the external body forces.

Finally we get to the definition of dynamically similar fluids.

**Definition 1.13.** Given two fluids with the same geometry, we say they are dynamically similar if each has characteristic parameters $\mu$, $U$, $\rho_\infty$, $L$ and $\vec{g}$ such that their Reynolds and Froude numbers are equal.

This dynamical similarity means that their dimensionless equations of flow are equal and thus their flow's properties will evolve in the same way (given equivalent initial conditions).

**Proposition 1.14.** Dynamical similarity between fluids with the same geometry trivially constitutes an equivalence relation.

**Comment 1.** During this section we have not mentioned the Masss equation when talking about the evolution of the flow's properties. Note that we trivially have the same expression for the Mass equation (1.2) when we change to the dimensionless variables, for incompressible fluids.

**Comment 2.** The hypothesis that the flows have the same geometry is a necessary condition, as the evolution of the flow heavily depends on the boundary conditions. In most practical cases the geometries involved are different scales of the same problem, as stated in the beginning of the section.

## 1.4 Evolution of the properties of the fluid

In the previous sections we have showed the behavior of the velocity field of the flow, as this gives the evolution of the fluid's flow over the time interval. Nonetheless, in most practical applications it is also important to look at how other properties of the fluid may change over time (temperature, electrical conductivity, etc).

Given a general scalar property defined over a volume $\phi(\vec{x}, t)$, the change of this property over time in a certain region $\Sigma_t$ of the fluid is given by:

$$\frac{d}{dt}\int_{\Sigma_t}(\rho\phi)\,d\vec{x} = \int_{\Sigma_t}\left(\frac{\partial(\rho\phi)}{\partial t} + \vec{\nabla}(\rho\vec{u}\phi)\right)d\vec{x}$$

where we used the transport theorem. Now using physical arguments, the causes of the change of a property $\phi$ are given by two contributions: the rate of generation or destruction of the property, which can be represented by a source term $\dot{S}$; and the diffusion of the property in the boundaries of the region due to the change of the property value in the boundaries, which can be represented by the diffusive term $\vec{\nabla}(\Gamma\vec{\nabla}\phi)$ where $\Gamma$ is called the diffusion coefficient. Then the change of $\phi$ over a certain region $\Sigma_t$ is given by:

$$\frac{d}{dt}\int_{\Sigma_t}(\rho\phi)\,d\vec{x} = \int_{\Sigma_t}\dot{S}d\vec{x} + \int_{\partial\Sigma_t}\vec{\nabla}\phi\cdot\vec{n}\,dS = \int_{\Sigma_t}\left(\dot{S} + \vec{\nabla}(\Gamma\vec{\nabla}\phi)\right)d\vec{x}$$

where we used the divergence theorem in the last equality. As we took and arbitrary small region $\Sigma_t$ the equality holds for the integrands alone, and therefore we get the following expression which gives the evolution of $\phi$.

$$\frac{\partial(\rho\phi)}{\partial t} + \vec{\nabla}(\rho\vec{u}\phi) = \vec{\nabla}(\Gamma\vec{\nabla}\phi) + \dot{S}. \tag{1.18}$$

It is interesting to point out that this expression can also be applied to the velocity field components and so we get to the momentum equations component-wise.

Furthermore, from this point we can define the convective and diffusive behavior of a fluid property:

**Definition 1.15.** Given a fluid $\Omega_t$ $\forall t \in [0, T]$ and a scalar property of the fluid $\phi : \Omega \times [0, T] \longrightarrow \mathbb{R}$ we define the following behaviors of the property:

- $\vec{\nabla}(\rho\vec{u}\phi)$ we will call convective behavior or convective term of $\phi$.
- $\vec{\nabla}(\Gamma\vec{\nabla}\phi)$ we will call diffusive behavior or diffusive term of $\phi$.

Intuitively, the convective behavior of a property describes the way the property values change due to the fact that the fluid is moving (movement given by $\vec{u}$), while the diffusive behavior describes how the property values change due to the different values of the surrounding fluid particles (via diffusion).

In general practical applications, fluid properties like pressure $p(\vec{x}, t)$ and density $\rho(\vec{x}, t)$, that appear in the Navier-Stokes equations to determine the fluid flow, may be related to each other and to other properties (such as temperature in an equation of state). Therefore, in order to compute the fluid's flow it will also be necessary to compute how these properties change over time.

## 1.5 Helmholtz-Hodge Decomposition

In this section we will take a more profound look at the role of the pressure for incompressible homogeneous viscous fluids, as it leads to a very interesting result not only from a theoretical point of view but also for numerical applications. During this section we will assume ideal flow boundary conditions, we recall that the condition is $\vec{u} \cdot \vec{n} = 0$.

First, we start by presenting a general result of vector fields in $\mathbb{R}^n$ for $n = 2, 3$ that will be the main point of our argument:

**Theorem 1.16** (Helmholtz-Hodge Decomposition theorem)**.** Given a vector field $\vec{w}$ defined on an open region $\Sigma \subseteq \mathbb{R}^n$ for $n = \{2, 3\}$, this vector field can be uniquely decomposed in the following form:

$$\vec{w} = \vec{u} + \vec{\nabla} p \tag{1.19}$$

where p is a scalar field over $\Sigma$ and u is a vector field over $\Sigma$ that satisfies:

1. $\vec{\nabla} \cdot \vec{u} = 0$,
2. $\vec{u} \cdot \vec{n} = 0$, over $\partial\Sigma$.

*Proof.* In order to prove the uniqueness of the decomposition we show the orthogonality of $\vec{u}$ and $\vec{\nabla} p$ over the region $\Sigma$. We have that:

$$\vec{\nabla}(\vec{u}p) = (\vec{\nabla} \cdot \vec{u})p + \vec{u}(\vec{\nabla} p) = \vec{u}(\vec{\nabla} p)$$

where the last equation follows from the free divergence condition 1. in the theorem statement. With this we can calculate the scalar product of $\vec{u}$ and $\vec{\nabla} p$ over the

region $\Sigma$ as follows:

$$\int_\Sigma \vec{\nabla} p \cdot \vec{u}\, d\vec{x} = \int_\Sigma \vec{\nabla}(p\vec{u})\, d\vec{x} = \int_{\partial\Sigma} (p\vec{u}) \cdot \vec{n}\, dS = 0$$

where we have used the divergence theorem to turn the integral over the region $\Sigma$ to an integral over the boundary of the region $\partial\Sigma$ and the condition $\vec{u} \cdot \vec{n} = 0$ of the theorem to get the last equation.

Using this result, if we have two decompositions $\vec{w} = \vec{u_1} + \vec{\nabla} p_1 = \vec{u_2} + \vec{\nabla} p_2$ then we have:

$$\vec{u_1} - \vec{u_2} + \vec{\nabla}(p_1 - p_2) = 0$$

By performing the inner product $(\vec{u_1} - \vec{u_2}) \cdot \left(\vec{u_1} - \vec{u_2} + \vec{\nabla}(p_1 - p_2)\right)$ over the region we get:

$$0 = \int_\Sigma \left[ \|\vec{u_1} - \vec{u_2}\|^2 + (\vec{u_1} - \vec{u_2})\vec{\nabla}(p_1 - p_2) \right] d\vec{x} = \int_\Sigma \|\vec{u_1} - \vec{u_2}\|^2\, d\vec{x}$$

where the last equation follows from the orthogonality relation. We then get that $\vec{u_1} = \vec{u_2}$ and thus the gradients of $p$ need to be equal $\vec{\nabla} p_1 = \vec{\nabla} p_2 \implies p_1 = p_2 + C$ where $C \in \mathbb{R}$ is an arbitrary constant. Therefore, the decomposition is unique (up to an additive constant with $p$).

Now let's prove the existence of the decomposition. We take a look at the divergence of the given vector field $\vec{w}$:

$$\vec{\nabla} \cdot \vec{w} = \vec{\nabla} \cdot \vec{u} + \vec{\nabla} \cdot \vec{\nabla} p = \Delta p$$

where we have used the free divergence of $\vec{u}$. Furthermore, we have that:

$$\vec{n} \cdot \vec{w} = \vec{n} \cdot \vec{u} + \vec{n} \cdot \vec{\nabla} p = \vec{n} \cdot \vec{\nabla} p = \frac{\partial p}{\partial n}$$

From this two statements and a given vector field $\vec{w}$, we define a Neumann problem:

$$\Delta p = f := \vec{\nabla} \cdot \vec{w} \;\; over \;\; \Sigma \;\; and \;\; \frac{\partial p}{\partial n} = g := \vec{n} \cdot \vec{w} \;\; over \;\; \partial\Sigma$$

which is known to have a solution (see [8]) $p$ up to an additive constant if, and only if:

$$\int_\Sigma f\, d\vec{x} = \int_{\partial\Sigma} g\, dS$$

which holds due to the divergence theorem. From this solution we define $\vec{u} = \vec{w} - \vec{\nabla} p$, that has the desired properties, and we get the desired decomposition.

□

From the theorem's proof we see that the gradient of the scalar field $p$ projects the vector field $\vec{w}$ into a divergence free vector field $\vec{u}$ that is also parallel to the boundary. Therefore, from the theorem we get the following corollary:

**Corollary 1.17.** We can define the projector operator $\Pi$ that projects a vector field over a region $\Sigma$ into a divergence free vector field parallel to the region boundary. That is:

$$\Pi(\vec{w}) = w - \vec{\nabla} p = \vec{u}$$

where $p$ is determined as specified in the theorem's proof.

By the Helmholtz-Hodge theorem this operator is well defined. Given a vector field $\vec{w}$ over $\Sigma$ and a divergence free vector field $\Pi(\vec{w}) = \vec{u}$ parallel to the region boundary, the operator has the following properties:

1. $\vec{w} = \Pi(\vec{w}) + \vec{\nabla} p$,
2. $\Pi(\vec{u}) = \vec{u}$,
3. $\Pi(\vec{\nabla} p) = 0$;

which can be easily proved using the theorem proof's arguments.

We can now apply this operator to our Momentum equation (1.17) (without external body forces) and get:

$$\Pi\left(\frac{\partial \vec{u}}{\partial t} + \frac{1}{\rho_\infty}\vec{\nabla} p\right) = \Pi\left(-(\vec{u}\cdot\vec{\nabla})\vec{u} + \frac{1}{Re}\Delta\vec{u}\right). \tag{1.20}$$

Recalling previous sections, we assumed $\vec{u}$ was a sufficiently smooth function, then it holds that:

$$\Pi(\vec{u}) = \vec{u} \Longrightarrow \Pi\left(\frac{\partial \vec{u}}{\partial t}\right) = \frac{\partial \vec{u}}{\partial t}.$$

By applying this together with the third property of the operator, mentioned above, we get:

$$\frac{\partial \vec{u}}{\partial t} = \Pi\left(-(\vec{u}\cdot\vec{\nabla})\vec{u} + \frac{1}{Re}\Delta\vec{u}\right). \tag{1.21}$$

This expression is an analogous decomposition to the one presented in the theorem but with $\vec{w} = -(\vec{u}\cdot\vec{\nabla})\vec{u} + \frac{1}{Re}\Delta\vec{u}$ and $\vec{u} = \frac{\partial \vec{u}}{\partial t}$. Consequently, the pressure gradient can be extracted as done in the theorem's proof by:

$$\vec{\nabla}\cdot\left(-(\vec{u}\cdot\vec{\nabla})\vec{u} + \frac{1}{Re}\Delta\vec{u}\right) = \Delta p$$

with

$$\frac{\partial p}{\partial n} = \vec{n} \cdot \left( -(\vec{u} \cdot \vec{\nabla})\vec{u} + \frac{1}{Re}\Delta\vec{u} \right).$$

In the same way we did for a general property $\phi$ in the previous section, we will define the following terms:

**Definition 1.18.** Given an incompressible homogeneous viscous fluid $\Omega_t$ for $t \in [0, T]$ with a fluid flow given by the velocity field $\vec{u}$, we define its convective-diffusive behavior as the term:

$$R(\vec{u}) = -(\vec{u} \cdot \vec{\nabla})\vec{u} + \frac{1}{Re}\Delta\vec{u}$$

where $-(\vec{u} \cdot \vec{\nabla})\vec{u}$ is the convective term and $\frac{1}{Re}\Delta\vec{u}$ is the diffusive term.

We can then rewrite the decomposition of the Momentum equation (1.21) with this convective-diffusive term:

$$\frac{\partial \vec{u}}{\partial t} = \Pi(R(\vec{u})) \quad with \quad \Delta p = \vec{\nabla} \cdot R(\vec{u}) \tag{1.22}$$

To sum up, we have derived and expression of the Momentum equation of incompressible homogeneous viscous fluids which does not depend on the pressure. Moreover, we have seen that in this case, the pressure is uniquely determined by the incompressibility condition $\vec{\nabla} \cdot \vec{u} = 0$ as the function that projects the convective-diffusive term into the a divergence free term.

This result is the foundation for a variety of numerical solution schemes of the Navier-Stokes equations called Fractional Step or Projection methods.

# Chapter 2

# Discretization of a differential equation. Numerical solutions

Once we know how the change of the fluid flow and its properties are related by the differential equations, we proceed to the discretization of these behaviors in order to calculate how this magnitudes evolve with time . Our main goal is to transform a differential equation, written in terms of a function and its derivatives, into a system of equations in terms of the values of these functions in points of the fluid $\Omega_t$ $\forall t \in [0, T]$.

More specifically, given a fluid $\Omega_t \subseteq \Omega$ $\forall t \in [0, T]$, the first thing we need to do is discretize the fluid's particles themselves. To do this we set a grid of points over the fluids domain. During this section we will talk about fluids in $\mathbb{R}^2$ but the case in $\mathbb{R}^3$ is analogous.

Given a fixed $t \in [0, T]$, as $\Omega_t \subseteq \mathbb{R}^2$ we can use the Cartesian axis to define a grid of the fluid. Let $C = [a, b] \times [c, d] \subseteq \mathbb{R}^2$ denote the smallest rectangle such that $\Omega_t \subseteq C$ for this given time, then we can define:

**Definition 2.1.** Let $C = [a, b] \times [c, d]$ be a rectangle and $\{a_i\}_{i=0,...,r}$ and $\{c_j\}_{j=0,...,s}$ two finite partitions such that $a_0 = a$, $a_r = b$, $c_0 = c$, $c_s = d$. Then, we call a Cartesian grid of C the family of points

$$\{p_{i,j} = (a_i, c_j)\} \ \ where \ \ i = 0, ..., r; \ \ and \ \ j = 0, ..., s$$

As the shape of $\Omega_t$ will not be rectangular in general, we will have to distinguish between three types of point in our grid:

- Fluid points, which lie inside the fluid's domain, $p_{i,j} \in \Omega_t$;

- Obstacle points, which lie outside the fluid's domain and will not be accessible to the fluid, even for other $t \in [0, T]$ (solid walls or obstacles);
- Empty points, which lie outside the fluid's domain but could be accessed by the fluid for other $t \in [0, T]$ (empty space between fluid and obstacles).

The Navier-Stokes equations will only be considered for fluid points, and thus the discretized equations will only consider property values in this points.

Depending on the problem we may have the fluid enclosed in a fixed region, so there will not be empty points, called fixed boundary problems; or grid points that change as the fluid moves in the empty points, called free boundary problems.

We will only consider fixed boundary problems, where the points in the grid are either obstacle or fluid points. In addition, the obstacle points that are adjacent to a fluid point will be called boundary points. If some point of the grid lays in $\partial\Omega$ it will also be considered a boundary point.

**Comment 1.** If a free boundary problem is considered, the rectangle $C$ and its Cartesian grid may have to be recalculated $\forall t \in [0, T]$. However, another approach can be taken, by taking $C$ as the rectangle such that $\Omega_t \subseteq C \ \ \forall t \in [0, T]$.

On the other hand, in order to calculate the properties of the fluid flow for the time interval $[0, T]$ we must also discretize this interval. That is to give a finite partition of the time interval $\{t_i\}_{i \in \{0,\dots,k\}}$ such that $t_0 = 0$ and $t_k = T$ and calculate the values of the properties, and it's derivatives, at each time in the partition. A common practice, that we will also use, is to take uniform time steps between the elements of the partition, that is $\delta t = t_{i+1} - t_i = constant \ \forall i \in \{0, ..., k-1\}$.

In the following sections, we will see two spatial discretization schemes: the finite difference discretization and the control volume discretization; and define explicit and implicit temporal discretizations. In all sections we will consider two dimensional fixed boundary problems (for the three dimensional problem is analogous).

## 2.1 Finite difference discretization

One of the more straightforward methods to discretize differential equations is to write the derivatives of a function in terms of the finite difference of the values of the functions in different points. More accurately, we can derive a discretized

formulation of the derivatives of a function by using the Taylor series.

In one dimension, given a differentiable function $f : \mathbb{R} \to \mathbb{R}$ and three consecutive points $x_1$, $x_2$ *and* $x_3$ with a uniform spacing $h = x_2 - x_1 = x_3 - x_2$ we have:

$$f(x_1) = f(x_2) - h\left(\frac{df}{dx}\right)_{x_2} + \frac{h^2}{2}\left(\frac{d^2f}{dx^2}\right)_{x_2} - \frac{h^3}{6}\left(\frac{d^3f}{dx^3}\right)_{x_2} + \ ...$$

$$f(x_3) = f(x_2) + h\left(\frac{df}{dx}\right)_{x_2} + \frac{h^2}{2}\left(\frac{d^2f}{dx^2}\right)_{x_2} + \frac{h^3}{6}\left(\frac{d^3f}{dx^3}\right)_{x_2} + \ ...$$

By truncating in the third order term of the Taylor series and isolating the derivative terms we can obtain the following expressions, using the notation $f_i = f(x_i)$:

$$\left(\frac{df}{dx}\right)_{x_2} = \frac{f_3 - f_1}{2h} \ \ and \ \ \left(\frac{d^2f}{dx^2}\right)_{x_2} = \frac{f_3 + f_1 - 2f_2}{h^2}.$$

These expressions are the discretized versions of the first and second derivatives of $f$. In order to get expressions of higher accuracy order, one may truncate in higher order terms of the Taylor series and use the series of farther neighbor points around the desired point $x_2$ to isolate the derivatives.

In a more general sense, for a a function $u : \mathbb{R}^2 \to \mathbb{R}$ we can get the derivatives in an analogous way. For instance, in a two dimensional grid around a point $(x_i, y_j)$ whose neighbor points use the notation $(x_{i\pm1}, y_{j\pm1})$, and with spacing $h$ and $k$ in the direction x and y respectively, we get:

$$\left(\frac{\partial u}{\partial x}\right)_{(x_i,y_j)} = \frac{u_{(i+1,j)} - u_{(i-1,j)}}{2h} \ \ and \ \ \left(\frac{\partial^2 u}{\partial x^2}\right)_{(x_i,y_j)} = \frac{u_{(i+1,j)} + u_{(i-1,j)} - 2u_{(i,j)}}{h^2}$$

$$\left(\frac{\partial u}{\partial y}\right)_{(x_i,y_j)} = \frac{u_{(i,j+1)} - u_{(i,j-1)}}{2k} \ \ and \ \ \left(\frac{\partial^2 u}{\partial y^2}\right)_{(x_i,y_j)} = \frac{u_{(i,j+1)} + u_{(i,j-1)} - 2u_{(i,j)}}{k^2}.$$

And then the mixed partial derivatives are written in the following way:

$$\left(\frac{\partial^2 u}{\partial x \partial y}\right)_{(x_i,y_j)} = \frac{\frac{\partial u}{\partial y}_{(x_{i+1},y_j)} - \frac{\partial u}{\partial y}_{(x_{i-1},y_j)}}{2h} = ...$$

$$= \frac{u_{(i+1,j+1)} - u_{(i+1,j-1)} - u_{(i-1,j+1)} + u_{(i-1,j-1)}}{4hk}.$$

In the same way, one could find higher order derivatives with arbitrary accuracy order for all the points of the discretized domain. By substituting the discretized expressions of the derivatives in a differential equation we get the discretized equation.

### 2.1.1 Advantages and disadvantages

Regarding the benefits of this discretization method, it is an easy method to implement, as the general expression for a discretized derivative on a grid point $p$ in an arbitrary accuracy order, for a uniform spacing grid, can be expressed as:

$$\left(\frac{\partial^n f}{\partial x^n}\right)_p = \frac{\sum a_q f(q)}{h^n}$$

where the summation is done over the neighbors of p relevant to the accuracy order chosen, and the coefficients $a_q$ are tabulated in the literature. This expression is valid for all differential equations and so it makes discretization of multiple equations easier.

Nevertheless, one of the main disadvantages of the finite difference approach is that it has an intrinsic error given by truncating the Taylor series. For example, for the one dimensional problem, the truncation error of the derivative of a scalar function $f$, with accuracy order n, can be represented by:

$$O_n(x+h) = \frac{f^{(n+1)}(\zeta)}{(n+1)!}h^{n+1} \text{ where } x < \zeta < x+h$$

where this term is given by the Cauchy remainder of a Taylor series of n terms. In some equations, in order to ensure the accuracy of the discretization, the spacing between the grid points used has to be really small (resulting in more points in which to calculate the function), making the method too computationally expensive.

Finally, one main technical disadvantage is that the function considered has to be differentiable in order for the Taylor series to be defined, which in the general discretizations case may be a restricting condition.

## 2.2 Control volume discretization

Another discretization method often used in computational fluid dynamics is the control volume method. This method takes each point in the grid and assigns to it a control volume around the point. The way to do this in the case of our Cartesian grid is as follows. Given a point $p_{i,j}$ with neighbors given by $p_{i\pm1,j\pm1}$:

- We choose a point in the segment that joins $p_{i,j}$ with one of its neighbors, for all neighbors. We will call this point interface point. For instance, take $x_{i-1,j} < x_w < x_{i,j}$ the interface point chosen for the west neighbor.

- Analogously choose $x_e$, $y_n$ and $y_s$ for the other neighbors.
- We assign the rectangle $C_{i,j} = (x_w, x_e) \times (y_s, y_n)$ as the control volume for the point $p_{i,j}$.

Note that the control volumes of adjacent points in the grid do not overlap but share a common edge of the rectangle, that is a common boundary of the control volume. Furthermore, the positions of the interface points are chosen arbitrary, and although there is a common practice to set them at half the way between the neighboring points, this position can vary from point to point and in different problems.

When we have assigned control volumes for all the points of the grid, the discretization of the differential equation is done by integrating the equation over each of the control volumes with the next set of assumptions:

- The variation of an integrated function inside the control volume $C_{i,j}$ has to be assumed, although it is generally given by the value of the function at the grid point $p_{i,j}$.
- The value of a function in the boundary of the control volume $\partial C_{i,j}$, shared with other control volumes (or boundary points), has to be calculated by an appropriate profile assumption from the values of the function in the control volumes that share that boundary. Different profiles in different situations give raise to different discretizations.

After integrating the equation over one of the control volumes we get the discretized equation over the volume, that only depends in the values of the properties inside the volume and the neighboring volumes and the profile assumptions made.

After the discretization over the control volume is done, one gets the discretized equations for the problem.

### 2.2.1 Advantages and disadvantages

One of the main advantages of this method, specially when talking about physical differential equations, is that the method implies the integral conservation of the functions or properties used in the equation. This means that either considering small control volumes or the whole domain of the function, the integrated functions satisfy the equation and thus we have an integral conservation of the

function or property.

For instance in our case this method ensures the mass conservation equation (1.7) even within the control volumes, which in turn ensures physical accuracy of the discretization, and thus of the solution.

The main disadvantage of the method is the assumption of the variation of the integrated function within the control volume and at its boundaries, which is particular to each function and situation and may even vary with the integration of the same function in different equations. This gives a wide range of possible profile assumptions that have to be considered for improvements in accuracy or computational efficiency.

For the examples of discretization of the following sections we will use the control volume discretization as our main discretization method, as it allows us more freedom of choice between different schemes by choosing different profile assumptions.

## 2.3 Temporal discretization

Special treatment has to be used for the discretization of time derivatives, as one only has information about the property in the previous time step and needs to get the vale of the property at the next time step. Given a time interval $[0, T]$ with a partition $\{t_i\}_{i=1,\dots,k}$ of uniform spacing $\delta t$, we will have in general the following structure for a differential equation of a function $u$ of first order on the temporal variable:

$$\frac{\partial u(\vec{x}, t)}{\partial t} = \psi(t, u(\vec{x}, t))$$

where the function $\psi(t, u(\vec{x}, t))$ is given by the problem.

For the discretization of the time derivative one can assume different profiles for the variation of $u$ with time, although we will assume a linear profile. Noting $u$ in a time $t = t_0 + \delta t$ as $u^t$ and around time $t_0$ as $u^{t_0}$ then we have:

$$\frac{\partial u}{\partial t} = \frac{u^t - u^{t_0}}{\delta t}.$$

One method to model the change of $\psi$ in the different time steps $t$ and $t_0$ is the $\theta-$method. Given a parameter $\theta \in [0, 1]$, we have the discretized equation:

$$\frac{u^t - u^{t_0}}{\delta t} = \theta\psi(t, u^t) + (1 - \theta)\psi(t_0, u^{t_0}).$$

Using this discretized equation and the value of $u(\vec{x},t)$ for time $t_0$, one can isolate and calculate the new value for $t = t_0 + \delta t$. The parameter $\theta$ determines the type of temporal discretization: for $\theta = 0$ we say it is an explicit method, as $u^t$ depends explicitly on $u^{t_0}$ only; whether for $\theta \neq 0$ we say it is an implicit method (for $\theta = 1$ we say it is fully implicit), as $u^t$ has to be isolated or computed numerically. It can be shown that implicit discretizations have better computational stability (see [9]) although explicit methods are simpler to implement computationally.

When applying this discretization together with the control volume spatial discretization, we can directly apply the temporal discretization given above or integrate over the time step to get:

$$\int_{t_0}^{t} \frac{\partial u}{\partial t}\, dt = \left(\frac{u^t - u^{t_0}}{\delta t}\right) \delta t = u^t - u^{t_0}$$

$$\int_{t_0}^{t} \psi(t,u)\, dt = \left[\theta\psi(t,u(\vec{x},t)) + (1-\theta)\psi(t_0,u(\vec{x},t_0))\right] \delta t$$

and get the discretized equations.

## 2.4 Control volume discretization example

In this section we will apply the control volume discretisation method to our study case, incompressible homogeneous viscous fluids. We will consider the problem only in two dimensions due to notation simplicity, as the three dimensional problem is analogous. Given the velocity field of a fluid at each time by $\vec{u}(\vec{x},t)$, we recall the evolution of a general property $\phi$ in a incompressible fluid is given by:

$$\frac{\partial(\rho\phi)}{\partial t} + \vec{\nabla}(\rho\vec{u}\phi) - \vec{\nabla}(\Gamma\vec{\nabla}\phi) = S. \tag{2.1}$$

For this example we will consider $S = 0$ and $\Gamma$ to be an arbitrary constant. We can rewrite the equation as:

$$\frac{\partial(\rho\phi)}{\partial t} = \vec{\nabla}\left(\Gamma\vec{\nabla}\phi - (\rho\vec{u}\phi)\right) = \vec{\nabla}\cdot R(\phi) \tag{2.2}$$

where we have isolated the convective-diffusive transport terms of $\phi$.

Apart from this equation we recall the condition for the incompressible fluid velocity field $\vec{u}$:

$$\vec{\nabla}\cdot\vec{u} = 0. \tag{2.3}$$

Given a point $P$ of the grid, it's neighbors given by the notation $E$, $W$, $N$ and $S$ and the respective interface points given by the notation $e$, $w$, $n$ and $s$ where the

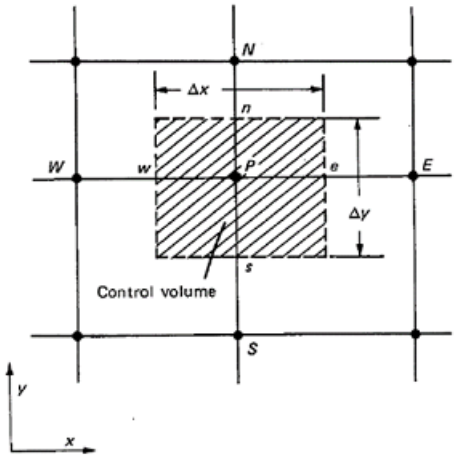


**Figure 2.1:** Example of the control volume around a grid point P, with the interface points located midway between the neighboring points.

interfaces are located midway between neighbor points (see diagram).

We integrate the two terms of the first differential equation over the control volume and over a time step from $t_0$ to $t = t_0 + \delta t$:

$$\int_{t_0}^{t} \int_V \frac{\partial(\rho\phi)}{\partial t}\, dV\, dt = \rho_\infty(\phi_P - \phi_P^0)\Delta x\, \Delta y$$

$$\int_{t_0}^{t} \int_V \vec{\nabla}\left(\Gamma\vec{\nabla}\phi - (\rho\vec{u}\phi)\right)\, dV\, dt = \int_{t_0}^{t} \int_{\partial V} \left(\Gamma\vec{\nabla}\phi - (\rho\vec{u}\phi)\right)\cdot\vec{n}\, dS\, dt$$

where we have used the fact that for incompressible homogeneous viscous fluids the density is constant in space and time, and the divergence theorem in the later part of the equation. Note that we use the notation $\phi$ for the property at time $t$ and $\phi^0$ for the property at time $t_0$.

Let's look at the calculation of the diffusive and convective terms separately.

### 2.4.1 Diffusive term discretization

For the diffusive term integral over the boundary of the control volume we assume that for each edge of the rectangle of the control volume the magnitudes are constant for the whole edge, and thus we have:

$$\int_{\partial V} (\Gamma\vec{\nabla}\phi)\cdot\vec{n}\, dS = \left[(\Gamma\vec{\nabla}\phi)_e - (\Gamma\vec{\nabla}\phi)_w\right]\Delta y + \left[(\Gamma\vec{\nabla}\phi)_n - (\Gamma\vec{\nabla}\phi)_s\right]\Delta x.$$

Now in order to get a discretized equation we have to assume a profile for $\vec{\nabla}\phi$. We assume a piecewise-linear profile for the change of $\vec{\nabla}\phi$ between points of the grid, and then we have:

$$(\Gamma\vec{\nabla}\phi)_e = \Gamma_e \frac{\phi_E - \phi_P}{\delta x_E}$$

where $\delta x_E$ is the distance between point $P$ and $E$.

For the diffusive coefficient $\Gamma$ a proper profile assumption has to be made too. A common approach is to take the harmonic mean of the coefficients $\Gamma_P$ and $\Gamma_E$ in relation with the position of the interface point $e$, given by the ratio $f_e = \frac{\delta x_e}{\delta x_E}$, where $\delta x_e$ is the distance from $P$ to $e$. Then we have:

$$\Gamma_e = \left(\frac{1 - f_e}{\Gamma_P} + \frac{f_e}{\Gamma_E}\right)^{-1}.$$

The correctness of this coefficient profile assumption can be physically argumented by looking at the flux transport of the property though the control volume boundary (see [4]).

### 2.4.2 Convective term discretization

As we did for the diffusive term, we assume the values of the convective term remain constant in every edge of the boundary of the control volume, then:

$$\int_{\partial V} (\rho\vec{u}\phi) \cdot \vec{n}\, dS = [(\rho\vec{u}\phi)_e - (\rho\vec{u}\phi)_w]\, \Delta y + [(\rho\vec{u}\phi)_n - (\rho\vec{u}\phi)_s]\, \Delta x$$

We calculate the integral over the boundary of the convective term for $\phi$ by assuming again a piecewise-linear profile for the convective term, then we have:

$$(\rho\vec{u}\phi)_e = \rho_\infty \vec{u}_e \frac{\phi_P + \phi_E}{2}$$

This profile assumption for the convective term is called central difference scheme. We will see in the later sections of computational examples some other schemes and their comparisons in performance for a given problem.

Note that the velocity in the interface point $\vec{u}_e$ denotes the projected component by the normal of the surface, given in the integral as $\vec{u} \cdot \vec{n}$. Therefore, $\vec{u}_e$ denotes the horizontal component of the velocity at the interface point.

### 2.4.3 Time step integration of convective diffusive term

For the integration of the convective-diffusive term over the time step $t_0 \rightarrow t_0 + \delta t$ we will use a fully implicit temporal discretization (where $\theta = 1$ as seen in

previous sections) then the diffusive-convective term integration ends up as:

$$\int_{t_0}^{t} \int_V R(\phi)\, dV\, dt = \int_V R(\phi) \delta t\, dV$$

where the magnitudes in $R(\phi)$ and the integrated terms ($\phi_P$, $\phi_E$ and so on) refer to the values for time $t = t_0 + \delta t$.

Aside from the discretization of equation (2.1) we have to discretize the incompressibility condition over the time step and the control volume:

$$\int_{t_0}^{t} \int_V \vec{\nabla} \cdot \vec{u}\, dV\, dt = \int_{\partial V} \vec{u} \cdot \vec{n}\, \delta t\, dS = \left( [\vec{u}_e - \vec{u}_w]\, \Delta y + [\vec{u}_n - \vec{u}_s]\, \Delta x \right) \delta t = 0 \qquad (2.4)$$

where the velocities $\vec{u}_{e,w,n,s}$ are the projected velocities by the normal to the boundary of the control volume at each edge. In addition, the velocities in the equation refer to the values for time $t = t_0 + \delta t$ (as we used a fully implicit temporal discretization).

Note that here we also made the assumption that the value of this velocity holds for the whole edge. In our study cases we will use this assumption often to simplify the calculations. The correctness of this assumption depends in the size of the control volumes and the real change in the velocities in this volumes. However, in our simple cases any error caused by this assumption can be reduced by taking a bigger number of smaller control volumes (finer grids with more grid points).

With this profile assumptions for the different terms in the integrals, we can finish the integration of the equations for the control volume. By using both equations we can rearrange the terms in a discretized equation, and get an equation of the following shape:

$$a_P \phi_P = a_E \phi_E + a_W \phi_W + a_N \phi_N + a_S \phi_S + a_{0P} \phi_P^0 + b$$

with $a_E = \frac{\Gamma_e \Delta y}{\delta x_E} + \frac{\rho_\infty \vec{u}_e \Delta y}{2}$ and analogously for $a_W$, $a_N$ and $a_S$; $a_{0P} = \frac{\rho_\infty \Delta x \Delta y}{\delta t}$; and $a_P = a_E + a_W + a_N + a_S + a_{0P}$. The term $b$ represents the discretized form of the source term $S$, which in general may not be $b = 0$ as it is in this example.

Together with the equation (2.4) that ensures incompressibilty, we have our system of discretized equations for each control volume.

In general for our study cases, we will always end up with a system of discretized equation of this form, with different expressions for the discretized coefficients (given by the profiles assumed in each case). Nevertheless, in the most

general case, where the velocity field is not given, we would also have a discretized equation of a similar form but with the velocity components. For each time step, we would first need to calculate the velocity field for the new time and then use this field to calculate the new values of the property.

## 2.5 Numerical solution of the discretized equations

Once we have discretized the considered differential equations, we have a system of equations with the unknown variables being the values of the properties and functions involved in the equation at certain finite number of points (given by the grid).

Once established the boundary conditions, in a discretized form, and the initial conditions for the first instant $t_0$, we have to solve the system, in our case of study that means give the numerical solution, in order to get the properties of the fluid in the next time step $t_1 = t_0 + \delta t$. By repeating this process we get the successive values of the properties in the whole discretized time interval $[0, T]$ and thus, the solution to our problem.

Although for each problem considered and each discretization method used the system of equations may vary, it is often a common practice to get a linear system of discretized equations such that the numerical solution of this equations is easily obtainable in most cases using numerical methods.

In our case of study we will only present one such method, that is the tridiagonal matrix algorithm (TDMA) for the resolution of linear systems of equations, and it's variation for the two dimensional case, the line-by-line tridiagonal matrix algorithm.

Given a point $P$ of the grid, it's neighbors given by the notation $E$, $W$, $N$ and $S$ and the respective interface points given by the notation $e$, $w$, $n$ and $s$ (see figure 2.1), we will end up with a discretized equation in the mentioned grid point for the property $\phi$ of the form:

$$a_P\phi_P = a_E\phi_E + a_W\phi_W + a_N\phi_N + a_S\phi_S + a_{0P}\phi_P^0 + b.$$

First, we will take a look at how the tridiagonal matrix algorithm works for a one dimensional line of points that follow a discretized equation:

$$a_P\phi_P = a_N\phi_N + a_S\phi_S + a_{0P}\phi_P^0 + b.$$

We redefine the coefficients and the points of the line in the following way:

$$a_i\phi_i = b_i\phi_{i+1}c_i\phi_{i-1} + d_i$$

where trivially $a_i = a_P$, $b_i = a_N$, $c_i = a_S$ and $d_i = a_{0P}\phi_P^0 + b$. The terms $i+1$ and $i-1$ reference the next and previous neighbors of the considered point $i \in \{0, ..., k\}$. We take the convention of $i = 0$ being the first point in the line, and therefore $c_0 = 0$, and $i = k$ the last point of the line, with $b_k = 0$. For the line we get the system of linear equations represented by the matrix:

$$\begin{pmatrix} a_0 & -b_0 & 0 & \cdots & & 0 & \\ -c_1 & a_1 & b_1 & \cdots & & 0 & \\ & \vdots & & \ddots & & \vdots & \\ & 0 & & \cdots & -c_{k-1} & a_{k-1} & -b_{k-1} \\ & 0 & & \cdots & 0 & -c_k & a_k \end{pmatrix}$$

which is a tridiagonal matrix. Furthermore, from the definition of $a_i = a_P = a_N + a_S + a_{0P}$ , $b_i = a_N$ and $c_i = a_S$ for $i = 0, ..., k$ we trivially see that the matrix is strict diagonal dominant, that is for a general matrix $(a_{ij})$:

$$|a_{ii}| > \sum_{j \neq i} |a_{ij}|$$

for every row. This ensures the stability of the numerical method and allows for Gaussian elimination without pivoting (for a precise characterization of the stability of the algorithm see [12]). To solve this system, using Gaussian elimination without pivoting, we look for the relation:

$$\phi_i = P_i\phi_{i+1} + Q_i$$

where $P_i$ and $Q_i$ can be obtained recursively as:

$$P_i = \frac{b_i}{a_i - c_iP_{i-1}}$$

$$Q_i = \frac{d_i + c_iQ_{i-1}}{a_i - c_iP_{i-1}}$$

where trivially we see $P_0 = b_0/a_0$, $Q_0 = d_0/a_0$ and $P_k = 0$. Then we get $\phi_k = Q_k$ and calculate back the values for the whole line. Furthermore, if the values in the last and first point are given by the boundary conditions, we can set $P = 0$ and $Q$ equal to the boundary condition value. Using this recursive method of calculating the coefficients and then calculating back the values of the points with the given relation, we get the solution of the system for the line. This is the numerical solution for the one dimensional problem.

Now let's take a look at how the line-by-line tridiagonal matrix algorithm works. For a given grid in a given time step $t_0 \to t = t_0 + \delta t$, we divide the grid into lines (or rows) (in our case following the Cartesian axis of the Cartesian grid) and we solve the set of discretized equations (set of linear equations) for the points of each line (row). For this, we assume the other values of the grid points outside the line (row) to be known from a previous iteration. Thus we can redefine:

$$d_i = a_E \phi_E + a_W \phi_W + a_{0P} \phi_P^0 + b$$

and we can use the TDMA algorithm in one dimension for each line (row) to get the updated values.

After repeating this process through the entire grid, all the grid points will have updated values. Then, we repeat the computations for each line (row) with the new updated values. We perform this iterative method until the property in each point does not differ from one iteration to the next (until the grid converges to the solution). This is called the line-by-line solution of the grid with the successive iterations until convergence. A sufficient condition for the convergence of this iterations is given by the Scaraborough criterion (see [11]):

$$\frac{\sum |a_{nb}|}{|a_P|} = \begin{cases} \leq 1 & \text{for all grid points} \\ < 1 & \text{for at least one grid point} \end{cases}$$

where the summation is done for all the neighbors of $P$ involved in the discretization equation (as all the not involved points have coefficient 0). In our studied cases, we ensure this condition by forcing the term $a_P$ to always follow the form:

$$a_P = \sum a_{nb} + a_{0P}$$

with $a_{0P} \geq 0$. Then all our numerical iterations will converge.

# Chapter 3

# Computational solutions of fluid flow properties

In this chapter we will look into two different simple examples of computational solutions for fluid properties. We will study the specific discretizations used in each method, and some variations in this discretizations and their consequences. In addition, we will compare the computational solutions we get with reference values for the specific problems.

It is important to note that in both examples we will consider incompressible homogeneous viscous fluids in two dimensions. Furthermore, instead of computing the fluid's properties for a given interval $[0, T]$ we will calculate the properties until their stationary state, that is until the property values in the grid from one time step to the next do not change.

The first exampe we are going to see is the two dimensional Convective-Diffusive transport of a general scalar property $\phi$. This example is equivalent to the control volume discretization example given in section (2.3) but this time we will consider different profile assumptions for the convective terms and discuss their consequences and the comparison with the reference values. In this example we will have a given fluid flow by the velocity field $\vec{u}$, specified in the problem.

The second example will by the computation of the fluid flow in a two dimensional square cavity where one edge of the cavity is moving at uniform speed (driven-cavity problem). For this case we will use the Helmholtz-Hodge decomposition theorem to implement a Fractional Step discretization method to get the velocity field $\vec{u}(\vec{x}, t)$.

## 3.1 Convective-Diffusive transport of a property

Given a rectangular domain $\Omega = [-1,1] \times [0,1]$ we have a fluid $\Omega_t = \Omega \ \forall t$. Given that the velocity field of this fluid is $\vec{u} = (u,v)$ where the components are specified by the function:

$$u(x,y) = 2y(1-x^2) \text{ and } v(x,y) = -2x(1-y^2)$$

that gives ideal fluid conditions in the boundaries $\{-1,1\} \times [0,1]$ and $[-1,1] \times \{1\}$ and inflow and outflow conditions in the boundary $[-1,1] \times \{0\}$ (see diagram of velocity field).

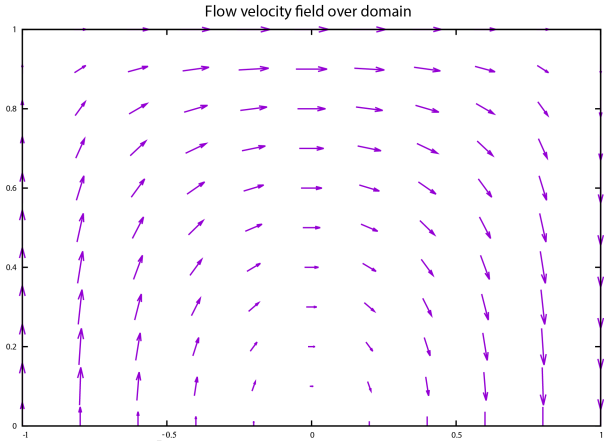


**Figure 3.1:** Diagram of the velocity field of the considered problem. Velocity vectors scaled for visual purposes

In addition, we have the following boundary conditions for the scalar property $\phi$:

$$\phi = 1 - \tanh[10] \text{ for } \begin{cases} x = -1,\ 0 \leq y \leq 1 \\ x = 1,\ 0 \leq y \leq 1 \\ -1 \leq x \leq 1,\ y = 1 \end{cases}$$

$$\phi = 1 + \tanh[10(2x+1)] \text{ for } -1 < x < 0 \ y = 0 \text{ (inlet)}$$

$$\frac{\partial \phi}{\partial n} = 0 \text{ for } 0 < x < 1 \ y = 0 \text{ (outlet).}$$

Note that the $\tanh[10(2x+1)]$ function present in the inlet boundary condition gives a $\phi \approx 0$ for $-1 < x < -0.5$ and $\phi \approx 2$ for $-0.5 < x < 0$. Moreover, the outlet condition tells us the value of the property at those points is equal to the value of the property in the points just above. At the other boundaries $\phi \approx 0$.

Finally, we have initial condition $\phi(x, y, 0) = 0 \; \forall (x, y) \in (-1, 1) \times (0, 1)$.

The numerical solutions of this problem will depend on the values we choose for the density $\rho_\infty$ and the diffusion coefficient $\Gamma$ (both constant for the whole fluid). Therefore, we will specify this parameters as the ratio $\frac{\rho_\infty}{\Gamma}$. We will later see in the discretization that this ratio is used in the calculation of the discretization coefficients. In addition, the reference values we have will depend on the parameter ratio used for the computation.

### 3.1.1 Discretization methods

We recall the behavior of the scalar property as defined in chapter 1 by (1.18):

$$\frac{\partial(\rho\phi)}{\partial t} = \vec{\nabla}(\Gamma\vec{\nabla}\phi - (\rho\vec{u}\phi)) + \dot{S} = \vec{\nabla} \cdot J + \dot{S}$$

with the ratio of generation of the property $\dot{S} = 0$ in this case. We proceed with the control volume discretization as we did in chapter 2:

$$\int_{t_0}^{t} \int_V \frac{\partial(\rho\phi)}{\partial t} \, dV \, dt = \rho_\infty(\phi_P - \phi_P^0)\Delta x \, \Delta y$$

$$\int_{t_0}^{t} \int_V \vec{\nabla} \cdot J \, dV \, dt = [(J_e - J_w)\Delta y + (J_n - J_s)\Delta y] \, \delta t$$

where we used fully implicit temporal discretization and constant value of $J$ in the boundary edges (as seen in chapter 2). However, we will not specify the profiles of the diffusive and convective terms yet.

We also discretize the incompressibility condition (as we did in chapter 2 in (2.4)):

$$\int_{t_0}^{t} \int_V \vec{\nabla} \cdot \vec{u} \, dV \, dt = \int_{\partial V} \vec{u} \cdot \vec{n} \, \delta t \, dS = [\vec{u}_e - \vec{u}_w] \, \Delta y + [\vec{u}_n - \vec{u}_s] \, \Delta x = 0.$$

This last equation is then equivalent to:

$$[F_e - F_w] \, \Delta y + [F_n - F_s] \, \phi_P \Delta x = 0$$

where $F = \rho_\infty \vec{u}$ represent the convective transport. By joining the two equations we get:

$$\frac{\rho_\infty(\phi_P - \phi_P^0)\Delta x \, \Delta y}{\delta t} = [(J_e - F_e\phi_P) - (J_w - F_w\phi_P)] \, \Delta y + [(J_n - F_n\phi_P) - (J_s - F_s\phi_P)] \, \Delta y$$

To apply to this expression different profile assumptions, we use the following general formulation for the discretization coefficients (as presented in [4]):

$$(J_e - F_e\phi_P) = a_E(\phi_P - \phi_E) \text{ and } (J_w - F_w\phi_P) = a_W(\phi_W - \phi_P)$$

For

$$a_E = D_e A(|P_e|) + max(-F_e, 0)\Delta y \text{ and } a_W = D_w A(|P_w|) + max(F_w, 0)\Delta y$$

where $D_e = \frac{\Gamma \Delta y}{\delta x_E}$ represents the diffusive transport discretization (assuming a linear profile) and $A(|P_e|)$ is a function depending on the Péclet number $P_e = \frac{F_e \Delta y}{D_e} = \frac{\rho_\infty \vec{u}_e}{\Gamma \delta x_E} \propto \frac{\rho_\infty}{\Gamma}$ that varies when using different convection schemes (profile assumptions for the convective term). We will call this function Péclet function. The Péclet number intuitively represent the dominance of the convective term (for high Péclet numbers) or the diffusive term (low Péclet).

Note that the definitions of the coefficients where done for specific interfaces but are equivalent for the others. Furthermore, in this discretization coefficients we see the dependence with the parameter ratio previously mentioned. With this general discretization coefficients we can present the general discretization equation:

$$a_P\phi_P = a_E\phi_E + a_W\phi_W + a_N\phi_N + a_S\phi_S + a_{0P}\phi_P^0.$$

With:

$$a_E = D_e A(|P_e|) + max(-F_e, 0)\Delta y \text{ and } a_W = D_w A(|P_w|) + max(F_w, 0)\Delta y$$

$$a_N = D_n A(|P_n|) + max(-F_n, 0)\Delta y \text{ and } a_S = D_s A(|P_s|) + max(F_s, 0)\Delta y$$

$$a_{0P} = \frac{\rho_\infty \Delta x \Delta y}{\delta t} \text{ and } a_P = a_E + a_W + a_N + a_S + a_{0P}$$

where the parameters involved are defined as mentioned above and the function $A(|P|)$ will change depending on the convection scheme used.

In our case we will use three different convection schemes: the central difference scheme (CDS) (with the hybrid correction), the upstream scheme and the quadratic upstream interpolation for convective kinematics scheme (QUICK scheme).

For the central difference scheme the variation of the property is taken to be linear between grid points. As we saw in the control volume example section (2.3) , we have:

$$\phi_e = \frac{1}{2}(\phi_E + \phi_P) \text{ and } \phi_w = \frac{1}{2}(\phi_P + \phi_W)$$

which lead to the discretization coefficients:

$$a_E = D_e - \frac{F_e}{2} \text{ and } a_W = D_w + \frac{F_w}{2}$$

which are the same coefficient we would obtain if we used $A(|P|) = 1 - 0.5|P|$. Therefore, this is the Péclet function associated with this convection scheme.

Nevertheless, by looking at the expression for the coefficients or the Péclet function we see that for sufficiently large $F$, that is large Péclet numbers (in fact for |P|>2) we would have negative discretization coefficients which would lead to unrealistic solutions and divergence of the numerical solutions (by Scarborough's criterion). For this reason we introduce the hybrid variation that makes the coefficient 0 whenever the Péclet number would make the coefficients negative. In our general formulation, this means taking $A(|P|) = max(0, 1 - 0.5|P|)$. We will see that this variation will make the CDS scheme converge to the upstream scheme for large Péclet numbers.

For the upstream or upwind scheme, we make the value of the property on the face $\phi_e$ equal to the value of the property at the grid point on the upstream side of the face, from where the velocity in the considered control volume transports the property. That is:

$$\phi_e = \phi_P \text{ for } F_e > 0$$
$$\phi_e = \phi_E \text{ for } F_e < 0$$

and equivalently for the other interfaces. This leads to the same coefficients as the ones we get with the Péclet function A(|P|)=1. This scheme takes into account the direction of the flow to calculate the convection term, whereas the central difference scheme calculated the average between the two grid points. Nevertheless, this scheme also leads to inaccuracies when the direction of the flow is not perpendicular to the chosen grid (see [4]).

Finally, the last scheme considered is the QUICK scheme, which is an upgrade of the upwind scheme where we calculate the property in an interface by doing a quadratic interpolation using the surrounding neighbor points (W and E) and the upstream second neighbors (WW or EE). Due to the quadratic interpolation, we will see this scheme has a better accuracy (higher order accuracy).

We get the following expressions for the quadratic interpolations (equivalent in the vertical direction N-S):

$$\text{For } F_e > 0 \text{ and } F_w > 0 \begin{cases} \phi_w = \frac{6}{8}\phi_W + \frac{3}{8}\phi_P - \frac{1}{8}\phi_{WW} \\ \phi_e = \frac{6}{8}\phi_P + \frac{3}{8}\phi_E - \frac{1}{8}\phi_W \end{cases}$$

$$\text{For } F_e < 0 \text{ and } F_w < 0 \begin{cases} \phi_w = \frac{6}{8}\phi_P + \frac{3}{8}\phi_W - \frac{1}{8}\phi_E \\ \phi_e = \frac{6}{8}\phi_E + \frac{3}{8}\phi_P - \frac{1}{8}\phi_{EE} \end{cases}$$

which gives the following coefficients:

$$a_W = D_w + \frac{6}{8}\alpha_w F_w + \frac{1}{8}\alpha_e F_e + \frac{3}{8}(1-\alpha_w)F_w$$

$$a_E = D_e - \frac{3}{8}\alpha_e F_e - \frac{1}{8}(1-\alpha_w)F_w - \frac{6}{8}(1-\alpha_e)F_e$$

$$a_{WW} = -\frac{1}{8}\alpha_w F_w \text{ and } a_{EE} = \frac{1}{8}(1-\alpha_e)F_e$$

where $\alpha = \begin{cases} 1 \text{ if } F > 0 \\ 0 \text{ if } F < 0 \end{cases}$.

Once more we have some discretization coefficients that could be negative, which could lead to unrealistic solutions and divergence of the numerical method. For this reason, we introduce a reformulation of the coefficients that can be used with iterative methods (presented in [12]) , where some of the values of the current coefficients will be thought of as part of the source term b calculated with the last known property values of the neighbors. When repeating this iterative method while updating this last known values we will converge to a solution. The modification of the QUICK scheme discretization coefficients is:

$$a_W = D_w + \alpha_w F_w \text{ and } a_E = D_e - (1-\alpha_e)F_e$$

$$b = \frac{1}{8}(3\phi_P - 2\alpha_W - \alpha_{WW})\alpha_w F_w + \frac{1}{8}(\phi_W + 2\phi_P - 3\phi_E)\alpha_e F_e +$$

$$+\frac{1}{8}(3\phi_W - 2\phi_P - \phi_E)(1-\alpha_w)F_w + \frac{1}{8}(\phi_{EE} + 2\phi_E - 3\phi_P)(1-\alpha_e)F_e.$$

We will see that this scheme adjusts very well to the real behavior of the problem, while giving fast convergence in the numerical solution. Nonetheless, for coarse grids we will see that it has some overshooting, the solution is larger than the real behavior; and undershooting, the solution is lower than the real behavior, around points of sudden change.

### 3.1.2 Numerical solution

As specified in the previous chapter, we will use a line-by-line TDMA numerical method to solve the linear discretized equations. However, it is important to note that for the last scheme, the QUICK scheme, we do not have a real tridiagonal matrix. However, we turn it into a tridiagonal matrix by using the modification (presented in [12]) introducing the second neighbors terms as known values in the independent term of each equation (b in the discretization equation). Iterations of the solver make the values converge to the solution.

### 3.1.3 Convection scheme comparison

Although we will compute the property values for the whole domain until the stationary state, to evaluate the numerical solutions for the different parameters and schemes we will compare the temperatures at the outlet boundary (at $y = 0$ and $0 \leq x \leq 1$). The reference values are specified in the following table (reference values from [13]):

| Position x | $\rho/\Gamma = 10$ | $\rho/\Gamma = 10^3$ | $\rho/\Gamma = 10^6$ |
|---|---|---|---|
| 0.0 | 1.989 | 2.0000 | 2.000 |
| 0.1 | 1.402 | 1.9990 | 2.000 |
| 0.2 | 1.146 | 1.9997 | 2.000 |
| 0.3 | 0.946 | 1.9850 | 1.999 |
| 0.4 | 0.775 | 1.8410 | 1.964 |
| 0.5 | 0.621 | 0.9510 | 1.000 |
| 0.6 | 0.480 | 0.1540 | 0.036 |
| 0.7 | 0.349 | 0.0010 | 0.001 |
| 0.8 | 0.227 | 0.0000 | 0.000 |
| 0.9 | 0.111 | 0.0000 | 0.000 |
| 1.0 | 0.000 | 0.0000 | 0.000 |

**Table 3.1:** Table holding the reference values for the outlet profile of $\phi$ using different parameter ratios $\rho/\Gamma$

Since we have reference values that depend on the Péclet number given by the relation $\rho/\Gamma$, when we refer in the following discussion to low or high Péclet numbers (and use notation P) we will be referring to low or high values for the ratio $\rho/\Gamma$.

For low Péclet numbers, the diffusive transport rate is dominant over the convective transport rate, and so we expect to find more uniformly decreasing values for the property at the outlet (typical of diffusive behavior). Alternatively, for large Péclet numbers we expect to find uniform values of the property where the flow (given by the velocity field) transports the inlet property values. As the flow draws semicircles form the inlet to the outlet (as seen in the velocity vector diagram), we expect to find uniform values of almost $\phi \approx 2$ at $0 \leq x \leq 0.5$ and $\phi \approx 0$ at $0.5 \leq x \leq 1.0$ (due to the inlet boundary condition).

For a grid with 3200 points (80x40 points) we have the following data from the different schemes and the reference values (see diagrams).

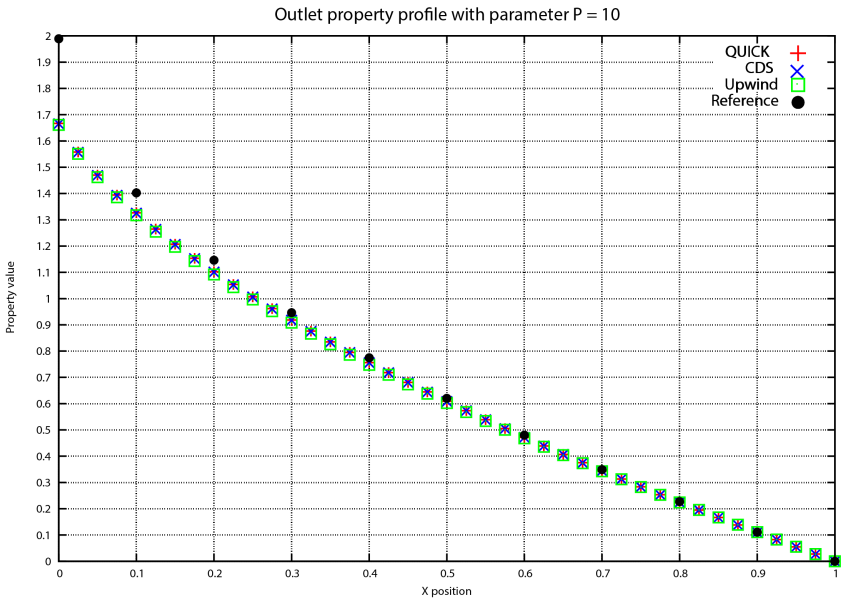


**Figure 3.2:** Plot of the property profile at the oultet boundary for $P = 10$ for different convection schemes with reference values. Grid of 3200 points (80x40).

We can clearly see (in figure 3.2) the expected uniformly decreasing behavior of the profile, given by the diffusive behavior for low Péclet numbers such as P=10. Moreover, we see that there is no clear difference between the different convection schemes. This follows from the fact that for such low Péclet numbers the convective behavior, and therefore the scheme used to describe it, is not dominant. However, we see that the initial value of the property (at x=0) is very different from the numerical values obtained. We will see in the following sections that this is due to the grid refinement and improves with finer grids. Finally, even with finer grids the behavior of the different schemes does not differ greatly, which supports the argument given previously.

In the case with $P = 10^3$ (figure 3.3) we start to see the expected behavior for large Péclet numbers, nearly uniform property values for the interval $0 \leq x \leq 0.5$ and really low values in the later profile. Nonetheless, with this parameter value we can also see the difference of the convection schemes, the QUICK scheme giving an almost perfect adjustment to the reference behavior while the CDS hybrid and upwind schemes fall behind. Still, the CDS hybrid scheme seems to adjust a little better than the upwind scheme. On the other hand, for the QUICK scheme we start to appreciate some slight overshooting and undershooting around the sudden change point ($x = 0.5$) as expected.

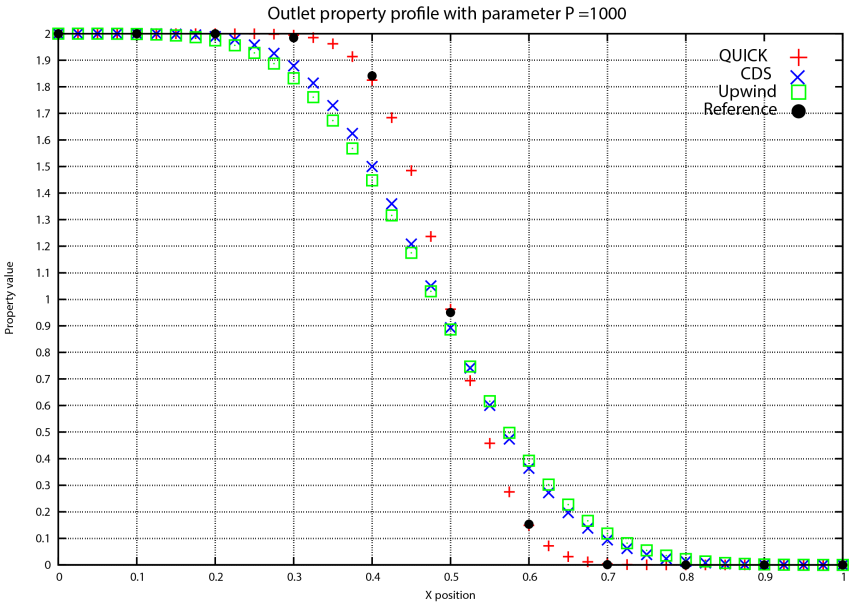


**Figure 3.3:** Plot of the property profile at the oultet boundary for $P = 10^3$ for different convection schemes with reference values. Grid of 3200 points (80x40).

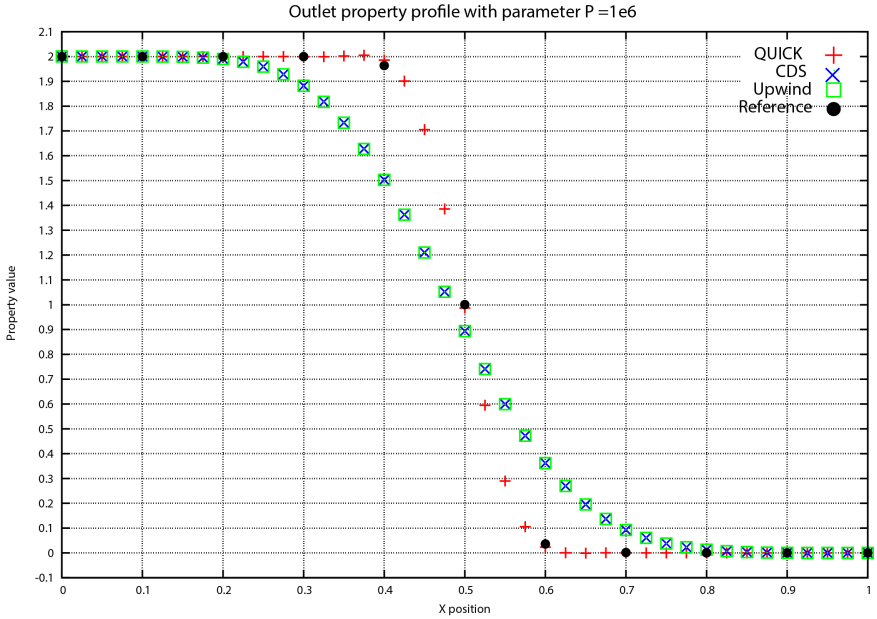


**Figure 3.4:** Plot of the property profile at the oultet boundary for $P = 10^6$ for different convection schemes with reference values. Grid of 3200 points (80x40).

With Péclet number $P = 10^6$ (figure 3.4) we can see without a doubt the expected plateau behavior in the first half of the profile and almost zero in the later half, with an almost perfect adjustment to the reference values for the QUICK scheme. Nevertheless, we now see some clear overshooting and undershooting in this scheme, although it will become clearer in the following section. With regards to the other schemes, we confirm that they do not adjust to the reference values as well as the QUICK scheme. In addition, we see that there is not much difference between CDS hybrid and upwind scheme for such large Péclet numbers.

After looking at the profiles for different values of the Péclet number we can conclude that the QUICK scheme adjusts best to the reference behavior, while the CDS hybrid and upwind scheme give almost equal, and worse, adjustments. This result was to be expected, as the QUICK scheme is an upgrade of the upwind scheme with higher order accuracy. More so, the coincidence between upwind and CDS hybrid is due to the hybrid correction of the CDS that makes them more similar for higher Péclet numbers while more different for average Péclet numbers, as seen in the $P = 10^3$ and $P = 10^6$ plots.

### 3.1.4 Grid refinement

Once established that the QUICK scheme is the best adjusting convection scheme over the ones considered, we will try this scheme with coarser and finer grids in order to see the effects of the grid refinement over the scheme. We will compare grids with 50 (10x5), 200 (20x10), 800 (40x20), 3200 (80x40) and 12800 (160x80) points, with the two different Péclet numbers $P = 10$ and $P = 10^6$.

For low Péclet numbers (like $P = 10$ in figure 3.5) we see that the behavior does not change much, other than better adjusting to the reference for finer grids (as expected). However, we see that the value of the first point of the profile ($x = 0$) converges clearly to the reference value for finer grids, although reaching this reference value means computing a much finer grid which in turn means some great computation time. Therefore, we will not reach that number of points in this report.

With large Péclet ($P = 10^6$ in figure 3.6) we have unrealistic values for coarse grids (50 pt., 200 pt. and 800 pt.), as there is clear overshooting and undershooting, which do not give realistic solutions. The perfect adjustment comes from 3200 pt. on.

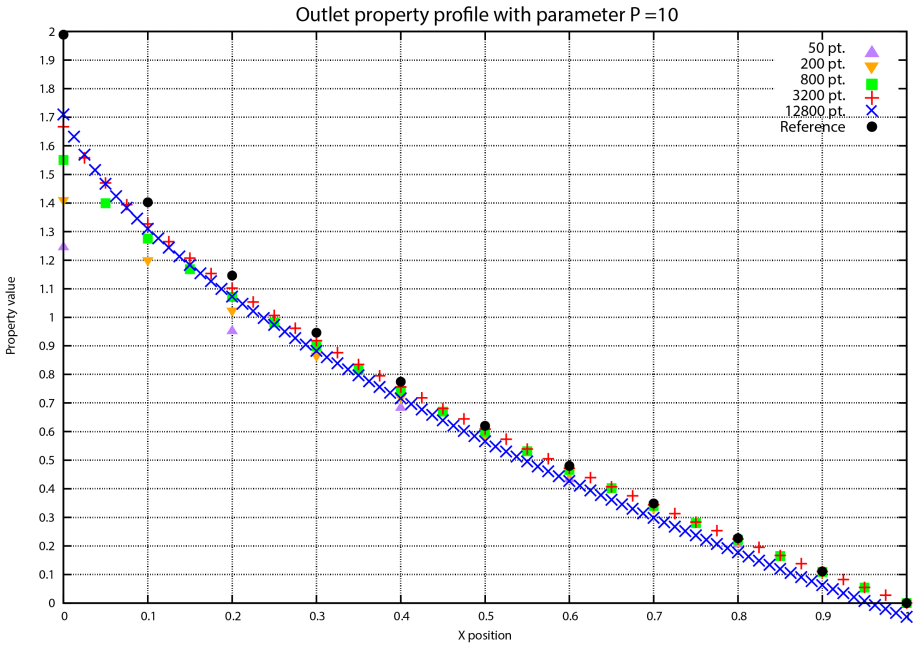


**Figure 3.5:** Plot of the property profile at the oultet boundary for $P = 10$ with QUICK convection scheme and reference values, for different grid point numbers.

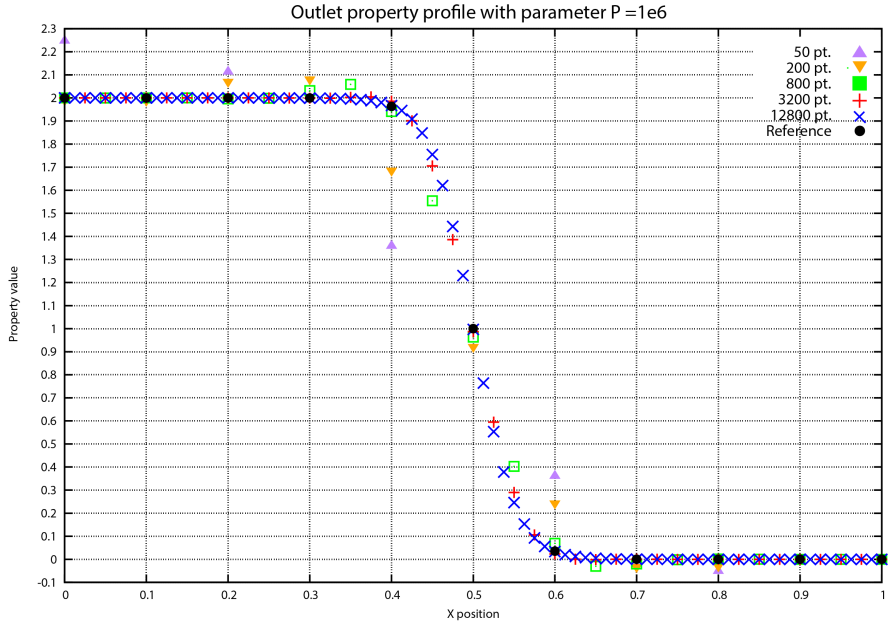


**Figure 3.6:** Plot of the property profile at the oultet boundary for $P = 10^6$ with QUICK convection scheme and reference values, for different grid point numbers.

It is also important to note that the number of points needed to get a perfect adjustment for low or large Péclet numbers is really different that the one needed for higher Péclet numbers. This difference arises from the fact that the QUICK convection scheme used is more accurate to the real case for large numbers, when the convective term is dominant over the diffusive term, as opposed to the case of low numbers, were the dominant term is the diffusive one. To lower the number of points in the grid needed to get a perfect adjustment for lower Péclet numbers we should discretize the diffusion term with a higher accuracy order profile (as for instance a quadratic interpolation of neighbors). However, we will not study this in our case.

With this we finish the study of our first computational example of the Convection-Diffusion transport of a scalar property $\phi$.

## 3.2 Fluid flow driven-cavity problem

Given a square domain $\Omega = [0,1]^2$ , we have a fluid $\Omega_t = \Omega \ \forall t$ with ideal fluid no-slip boundary conditions $\vec{u} = (0,0)$ in the left, right and lower boundaries ($\{0,1\} \times [0,1]$ and $[0,1] \times \{0\}$) and ideal fluid free-slip condition $\vec{u} = (1,0)$ in the upper boundary ($[0,1] \times \{1\}$). In addition, we have initial values $\vec{u}(x,y,0) = (0,0)$, $p(x,y,0) = 1000$ (arbitrary constant as the pressure is determined up to a constant) $\forall (x,y) \in (0,1)^2$ and no external body forces $\vec{g} = 0$.

With this boundary and initial conditions given for our problem, the only parameter that will affect this fluid's flow in the incompressible homogeneous viscous fluid conditions will be the Reynolds number. Therefore, our goal is to find the velocity field in the stationary state of the problem, and comparing it to the reference values, for different values of the Reynolds number associated with this fluid.

### 3.2.1 Fractional Step method

We recall the Navier-Stokes equations for incompressible homogeneous viscous fluids given by (1.17) and the incompressibility condition:

$$\frac{\partial \vec{u}}{\partial t} = R(\vec{u}) - \frac{1}{\rho_\infty} \vec{\nabla} p$$

$$\vec{\nabla} \cdot \vec{u} = 0$$

As seen in section (1.5) we can interpret the role of the pressure in this case as the projection of the time derivative of $R(\vec{u})$ into a divergence free vector. Then we have:

$$\frac{\partial \vec{u}}{\partial t} = R(\vec{u}) - \vec{\nabla} p \text{ where } \Delta p = \vec{\nabla} \cdot R(\vec{u})$$

In order to get the control volume discretization we must integrate over the control volume. However, we first discretize the time dependence. We use the notation $\vec{u}^t$ to denote the velocity at time $t$, and the same notation for other properties. For the time derivative of the velocity we have a linear profile, such that we have:

$$\frac{\partial \vec{u}}{\partial t}^{t+\delta t} = \frac{\vec{u}^{t+\delta t} - \vec{u}^t}{\delta t}.$$

For the convective-diffusive term $R(\vec{u})$ we use an explicit finite difference second order backwards method (as it depends in the two previous time steps)[1], and get:

$$R(\vec{u})^{t+\delta t} = \frac{3}{2} R(\vec{u})^t - \frac{1}{2} R(\vec{u})^{t-\delta t}.$$

Finally, for the pressure we assume a fully implicit discretization such that:

$$\left(\vec{\nabla} p\right)^{t+\delta t} = \vec{\nabla}(p^{t+\delta t}).$$

With this temporal discretization we can isolate the velocity at the next time step $\vec{u}^{t+\delta t}$ to get:

$$\vec{u}^{t+\delta t} = \vec{u}^t + \delta t \left( \frac{3}{2} R(\vec{u})^t - \frac{1}{2} R(\vec{u})^{t-\delta t} \right) + \delta t \vec{\nabla} p^{t+\delta t}$$

where we impose that the velocities satisfy the incompressibility condition (as we have an incompressible fluid). Then:

$$\vec{\nabla} \cdot \vec{u}^{t+\delta t} = 0$$

By the Helmholtz-Hodge decomposition theorem, there exist a unique decomposition of a vector $\vec{w}$ into a divergence free vector and a gradient of a scalar function, such that $\vec{w} = \vec{u} + \vec{\nabla} p$. Applying the theorem to the previous equation we get the unique decomposition:

$$\vec{u}^p = \vec{u}^{t+\delta t} + \vec{\nabla} \widetilde{p}$$

[1] This profile assumption is technically called explicit second-order Adams-Bashforth scheme.

where

$$\vec{u}^p = \vec{u}^t + \delta t \left( \frac{3}{2} R(\vec{u})^t - \frac{1}{2} R(\vec{u})^{t-\delta t} \right)$$

is called predictor velocity, and $\widetilde{p} = \delta t p^{t+\delta t}$ is a pseudo-pressure. Moreover, from the theorem we also know that the pseudo-pressure is determined by the Poisson equation:

$$\vec{\nabla} \cdot \vec{u}^p = \Delta \widetilde{p}.$$

To sum up, we have develop a way to calculate the velocity in a given time step $\vec{u}^{t+\delta t}$ by performing:

- Calculate the predictor velocity $\vec{u}^p$ explicitly from $\vec{u}^t$ and the convection-diffusion term at time $t$ and $t - \delta t$.
- Calculate the pseudo-pressure from the Poisson equation involving the predictor velocity.
- Calculate $\vec{u}^{t+\delta t} = \vec{u}^p - \vec{\nabla} \widetilde{p}$.

This method of time discretization of the incompressible homogeneous viscous equation is called Fractional Step method, or Projection method. In the following section we develop how to discretize the method for our control volume discretization in our Cartesian grid.

### 3.2.2 Contol volume discretization

In order to give a control volume discretization for our Cartesian grid to implement a computational solution, we have to calculate three things: the predictor velocity over the control volume (convective-diffusive term over the control volume); the pseudo-pressure from the poisson equation using the predictor velocity; and the real velocity by projecting the predictor velocity with the pseudo-pressure.

However, from the last step we get one problem worth mentioning. Given a grid point with notation as the one used in section (2.3) and given that we have calculated the predictor velocities and pseudo-pressures in all the points $P$ of a grid $\vec{u}_P^p$ and $\widetilde{p}_P$ (from now on we will use $p$ for the pseudo-pressure and call it pressure to simplify notation), we calculate the real velocity at the point:

$$\int_V \vec{u}_P dV = \vec{u}_P \Delta x \Delta y = \int_V \left( \vec{u}_P^p - \vec{\nabla} p \right) dV = \vec{u}_P^p \Delta x \Delta y - \int_{\partial V} p \vec{n} \, dS$$

where we have used the divergence theorem. Now using a linear profile for the variation of the pressure over grid points (that is $\mathfrak{p}_e = \frac{p_P + p_E}{2}$) we get:

$$\vec{u}_P = \vec{u}_P^p - \frac{1}{\Delta x \Delta y} \left[ (\frac{p_E + p_W}{2}) \Delta y + (\frac{p_N + p_S}{2}) \Delta x \right].$$

In this last step we see the current problem with our discretization. By calculating in this way the velocities and the pressures, we get that the velocity in one point of the grid is influenced only by the pressures surrounding this point, without taking into consideration the pressure at the point. This expression allows checkerboard solutions (that is alternating two realistic but different pressure fields so that the central difference of two alternated points is physically realistic) for the pressure to be acceptable, even if they are not realistic (see diagram for an example).

For this reason, it is necessary to use a different way to calculate the velocity. One such method for fixing the checkerboard problem is using a staggered grid for the problem, calculating the pressure at the grid points as done until now $p_P$, and the velocities at the interface points $\vec{u}_e$.

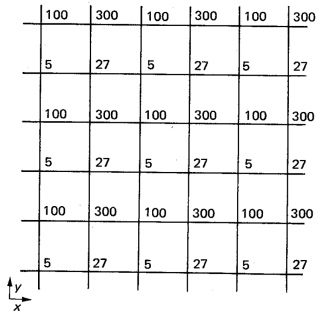


**Figure 3.7:** Diagram of an arbitrary checkerboard pressure field in two dimensions.

What is more, we can develop this fractional method component-wise $\vec{u} = (u, v)$ and then the horizontal components of the velocity will be calculated at the horizontal interfaces $u_e$ and $u_w$ and the vertical at the vertical interfaces $v_n$ and $v_s$. Then, we get the final step of the fractional method to be:

$$u_e = u_e^p - \frac{1}{\delta x_E}(p_E - p_P)$$

with no checkerboard problem. It is important to note that although the control volume for the pressure is the same as for the other examples, for each component of the velocity we have a staggered control volume, that we will take with the dimensions given by our Cartesian grid (see diagram of staggered control volumes).

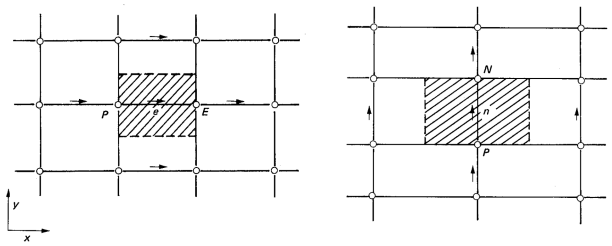


**Figure 3.8:** Diagram of the staggered grid with the staggered control volumes.

We also need the discretization of the term $R(u) = -(\vec{u} \cdot \vec{\nabla})u + \frac{1}{Re}\vec{\nabla} \cdot (\vec{\nabla}u)$

(and analogously $R(v)$), where we have both convective and diffusive terms. While the diffusive term gives no problem by using linear profiles for $\vec{\nabla}u$ (equivalently for $\vec{\nabla}v$) as we have already done in previous sections, special care has to be taken for the convective term.

We have $(\vec{u}\cdot\vec{\nabla})u = \vec{\nabla}(u\vec{u})$ by the incompressibility condition (for $\vec{u}$). Then the convective term discretization ends up as:

$$\int_V \vec{\nabla}(u\vec{u})\,dV = \int_{\partial V}(\vec{u}\cdot\vec{n})u\,dS = \left[(\vec{u}_E u_E) - (\vec{u}_W u_W)\right]\Delta y + \left[(\vec{u}_n u_n) - (\vec{u}_s u_s)\right]\delta x_E.$$

Note that we are handling $\vec{u}$ and $u$ differently: $\vec{u}$ is treated as a transporting velocity, transporting the scalar property $\phi = u$ which is treated as a transported velocity. For the profiles of the different velocities we have the following linear profile assumptions:

$$u_W = \frac{u_w + u_e}{2} = \vec{u}_W = \vec{u}\cdot\vec{n}_W \text{ but } u_n = \frac{u_{eN} + u_e}{2} \neq \vec{u}_n = \vec{u}\cdot\vec{n}_n = \frac{v_n + v_{nE}}{2}$$

where the notation $u_{eN}$ references the component $u_e$ of the north neighbor $N$, and $v_{nE}$ denontes the component $v_n$ of the east neighbor $E$ (neighbor notation from figure 2.1). The expressions work in the same way for the other components and interfaces. With this expressions we can denote the terms $R(u)$ and $R(v)$ in terms of the values of the staggered velocity grid and calculate the predictor velocity $\vec{u}^p = (u^p, v^p)$ explicitly without problems.

Finally, the only term we have left to discretize is the Poisson equation to determine the pressure $\Delta p = \vec{\nabla}(\vec{\nabla}p) = \vec{\nabla}\cdot\vec{u}^p$. Taking a control volume (not staggered) around the grid point $P$ we get:

$$\int_V \vec{\nabla}(\vec{\nabla}p)\,dV = \int_{\partial V}\vec{\nabla}p\cdot\vec{n}\,dS = \left[(\vec{\nabla}p)_e - (\vec{\nabla}p)_w\right]\Delta y + \left[(\vec{\nabla}p)_n - (\vec{\nabla}p)_s\right]\Delta x$$

$$\int_V \vec{\nabla}\cdot\vec{u}^p\,dV = \int_{\partial V}(\vec{u}^p\cdot\vec{n})\,dS = \left[u_e^p - u_w^p\right]\Delta y + \left[v_n^p - v_s^p\right]\Delta x$$

where we have done the projection $\vec{u}^p\cdot\vec{n}_e = u_e^p$ for all the interfaces. It is important to point out that in this last integral again we have remedied the checkerboard problem, as we have the specific velocity components at the interfaces directly due to the staggered grid. With this integration over the control volume we can obtain the discretized equation for the pressure:

$$a_P p_P = a_E p_E + a_W p_W + a_N p_N + a_S p_S + b.$$

with $a_E = \frac{\Delta y}{\delta x_E}$ and analogously for $a_W$, $a_N$ and $a_S$ and $a_P = a_E + a_W + a_N + a_S$. For the independent term we have the dependence on the predictor velocity, as $b = -\left(\left[u_e^p - u_w^p\right]\Delta y + \left[v_n^p - v_s^p\right]\Delta x\right)$.

### 3.2.3 Numerical solution

Although for the predictor velocity we do not need any special numerical method to get the values, as we have an explicit expression depending in the velocity values of the points in the staggered grid; we need a numerical solution for the Poisson equation of the pressure. As done in the previous example, we use a line-by-line TDMA method to solve the discretized equation.

For every time step, once we calculate the predictor velocity and solve the discretized pressure equation for the numerical solution of the pressure, we can calculate the new velocity field for the next time step. However, it is important to note that for the predictor velocity we will need the previous velocity field information to be stored, in particular the term $R(u)$ and $R(v)$ for $t - \delta t$. Trivially, for the first time step $0 \rightarrow \delta t$ the term $R(u)^{0-\delta t}$ will be treated as 0.

### 3.2.4 Results and comparison to reference values

Once performed the pertinent discretizations and numerical methods, we can present the solution velocity field in the stationary state for different values of the Reynolds number (see appendices with detailed vector field). For visualization purposes we will use constant grid size of 20x20 points.

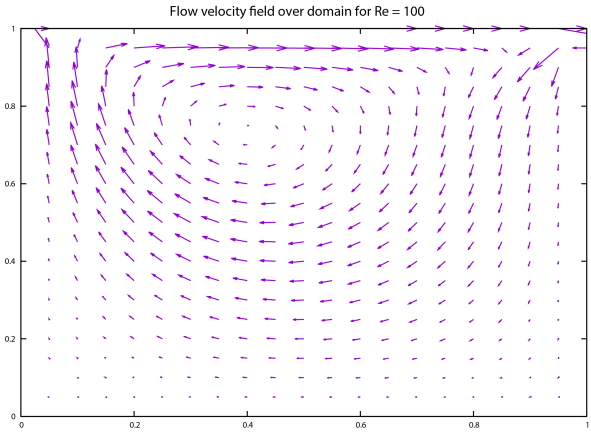


**Figure 3.9:** Diagram of the velocity vector field in the stationary state for the driven cavity example with $Re = 100$ in a grid of 400 points (20x20).

For small Reynolds numbers (such as $Re = 100$ in the first diagram) we see that the lid that moves (superior boundary) creates a vortex with center near the boundary. Nevertheless, this vortex smoothly diffuses over the inferior domain.

This is to be expected, as for low Reynolds number the viscous forces are more important, that is the diffusive term is more dominant than the convective term, and the velocities that create the vortex do not transport efficiently through the fluid. We will see how this changes for higher Reynolds numbers.

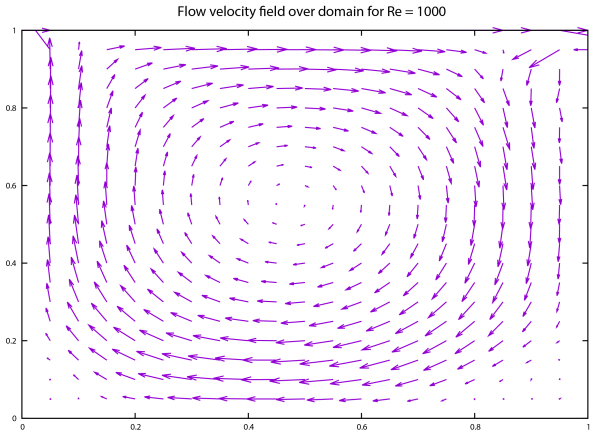


**Figure 3.10:** Diagram of the velocity vector field in the stationary state for the driven cavity example with $Re = 1000$ in a grid of 400 points (20x20).

For higher Reynolds numbers (for instance for $Re = 1000$ shown in the diagram) we clearly see a main vortex with center over the middle of the domain. Nonetheless, we see that the vortex still does not transport to the whole domain, as the inferior corner velocities remain almost 0.

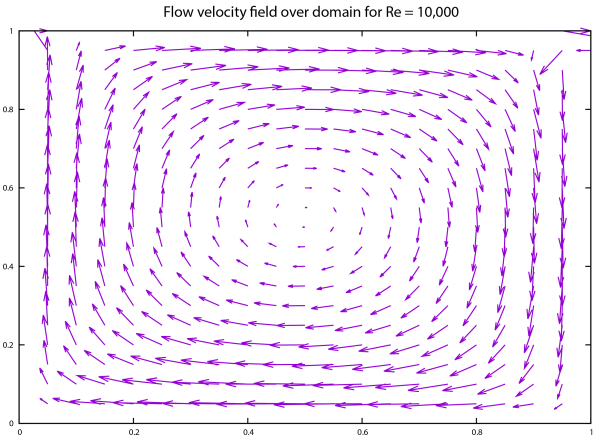


**Figure 3.11:** Diagram of the velocity vector field in the stationary state for the driven cavity example with $Re = 10,000$ in a grid of 400 points (20x20).

For even higher numbers (see diagram for $R = 10,000$) we see the same vortex as for the previous case, but in this case the vortex velocities have been transported to the whole domain. This is to be expected as for high Reynolds numbers the inertial forces are dominant, that is the convective term is more important than the diffusive term, and so the velocities of the lid that create the vortex are transported by these inertial forces to the whole domain.

It is important to note that in all cases the superior corners exhibit some singularities, that arise from the sudden change in boundary conditions between the walls of the corner, being $\vec{u} = 0$ for the left and right walls of the corners and $\vec{u} = (1, 0)$ for the superior wall. In addition, due to the small number of grid points (in order to visualize the flow properly) we can not see smaller turbulent behaviors of the flow in the corners that create secondary vortex in those areas (see appendix with detailed diagrams).

Aside from this qualitative study of the resulting fluid flow, we can compare the values of the velocity components with the reference values (which are specified in the appendix). We look at the horizontal component of the velocity at the bisection of the upper and lower walls, and at the vertical component of the velocity at the bisection of the left and right walls.

To compare with our computed data, we will use bilinear interpolation of the nearest grid points for each reference value, and calculate the mean squared absolute error, with the expression:

$$SqrErrU = \frac{1}{N}\sum_{i=0}^{N}(u_i - \overline{u_i})^2$$

where $u_i$ is the computed and interpolated value for the reference position, $\overline{u_i}$ is the reference value, and n is the number of reference values we have (in our case $n = 17$). The same expression applies to the component $v$. The results of the computed errors are shown for different numbers of grid points and Reynolds numbers (see table). The values for $Re = 10,000$ are only computed for a (20x20) grid and for a (40x40) grid, but not for a (80x80) grid due to excessive computation time. We choose to compute the values in this two grids in order to see the change in the error by refining the grid.

We clearly see that the mean squared error is much bigger for higher Reynolds than for lower, as was to be expected because more turbulence arises for higher Reynolds, with the secondary vortices arising near the corners. Because of this

| Re | 10 | | 1000 | | 10,000 | |
|---|---|---|---|---|---|---|
| Grid points | SqrErrU | SqrErrV | SqrErrU | SqrErrV | SqrErrU | SqrErrV |
| 400 (20x20) | $8.35\,10^{-4}$ | $6.57\,10^{-3}$ | $4.28\,10^{-2}$ | $6.64\,10^{-2}$ | $1.45\,10^{-1}$ | $1.68\,10^{-1}$ |
| 1600 (40x40) | $2.07\,10^{-4}$ | $3.67\,10^{-3}$ | $1.23\,10^{-2}$ | $3.70\,10^{-2}$ | $8.67\,10^{-2}$ | $9.29\,10^{-2}$ |
| 6400 (80x80) | $6.12\,10^{-5}$ | $3.01\,10^{-3}$ | $2.79\,10^{-3}$ | $2.21\,10^{-2}$ | - | - |

**Table 3.2:** Table showing the mean squared absolute error for the computed values of the velocities in the horizontal and vertical bisection lines over the geometric center.

singularities at the corners, the model used does not work well and propagates error to the numerical solution. Furthermore, we see that the vertical component of the velocity has more error, in general, than the horizontal one. This could be explained also by the appearance of the secondary vortices near the corners of the domain, that have greater effect over this component.

In general for all Reynolds numbers we see that the error is excessively large, in comparison with the magnitudes involved (velocities from 1 to 0). This is due to the numerical propagation of the error, that could be improved by using other numerical solution techniques, and to the grid points involved in the calculation. To support this last argument, we see that by using finer grids we decrease the error, for all Reynolds numbers. By using successively finer grids we could accomplish greater accuracy of the numerical solution. However, we will not check to this point for high Reynolds numbers due to the excessive computation time.

To sum up, we conclude this discretization method and numerical solution gives a good qualitative description of the fluid flow for both low and average Reynolds numbers, even for coarser grids. However, for high Reynolds numbers it fails to accurately show, even qualitatively, the effects of turbulence, even for finer grids. In addition, we conclude the numerical solution has deficient quantitative accuracy when comparing it to the reference values, either by numerical error propagation or model inaccuracy.

This ends our discussion of the second example of computational solution of fluid flow driven-cavity problem.

# Bibliography


[1] A.J. Chorin and J.E. Marsden, *A Mathematical Introduction to Fluid Mechanics*. Springer-Verlag, New York (2000).

[2] M. Griebel, T. Dornseifer and T. Neunhoeffer, *Numerical Simulation in Fluid Dynamics. A Practical Introduction*. Society for Industrial and Applied Mathematics, Philadelphia (1998).

[3] J.E. Marsden and T.J.R. Hughes, *Mathematical foundations of elasticity*. Dover Publications, New York (1994), ch. 2.

[4] S.V. Patankar, *Numerical Heat Transfer and Fluid Flow*. Hemisphere Publishing Corporation (1980).

[5] O.A. Ladyzhenskaya, *The Mathematical Theory of Viscous Incompressible Flow*. Gordon and Breach, New York (1969).

[6] J. Leray, *Sur le mouvement d'un liquide visqueux emplissant l'espace*. Acta Mathematica 63:1 (1934), pp. 193-248.

[7] C. Fefferman, *Existence and smoothness of the Navier-Stokes equations*. Clay Mathematics Institute.

[8] R. Courant and D. Hilbert, *Methods of Mathematical Physics*. Wiley-VCH (1953).

[9] P.A. Raviart and J.M. Thomas, *Introduction à l'analyse numérique des équations aux dérivées partielles*. Masson, Paris (1983), ch. 7.

[10] N.J. Higham, *Accuracy and Stability of Numerical Algorithms*. Society for Industrial and Applied Mathematics, Philadelphia (2002), ch. 9.

[11] J.B. Scarborough, *Numerical Mathematical Analysis*. Johns Hopkins Press, Baltimore (1955).

[12] T. Hayase, *A consistently formulated QUICK scheme for fast and stable convergence using finite-volume iterative calculation procedures*. Journal of Computational Physics 98:1 (1992), pp. 108-118

[13] R. Smith and A. Hutton, *The numerical treatment of advection: A performance comparison of current methods*. Numerical Heat Transfer 5:4 (1982), pp. 439-461

# Appendix 1: Detailed velocity field diagrams for driven-cavity problem

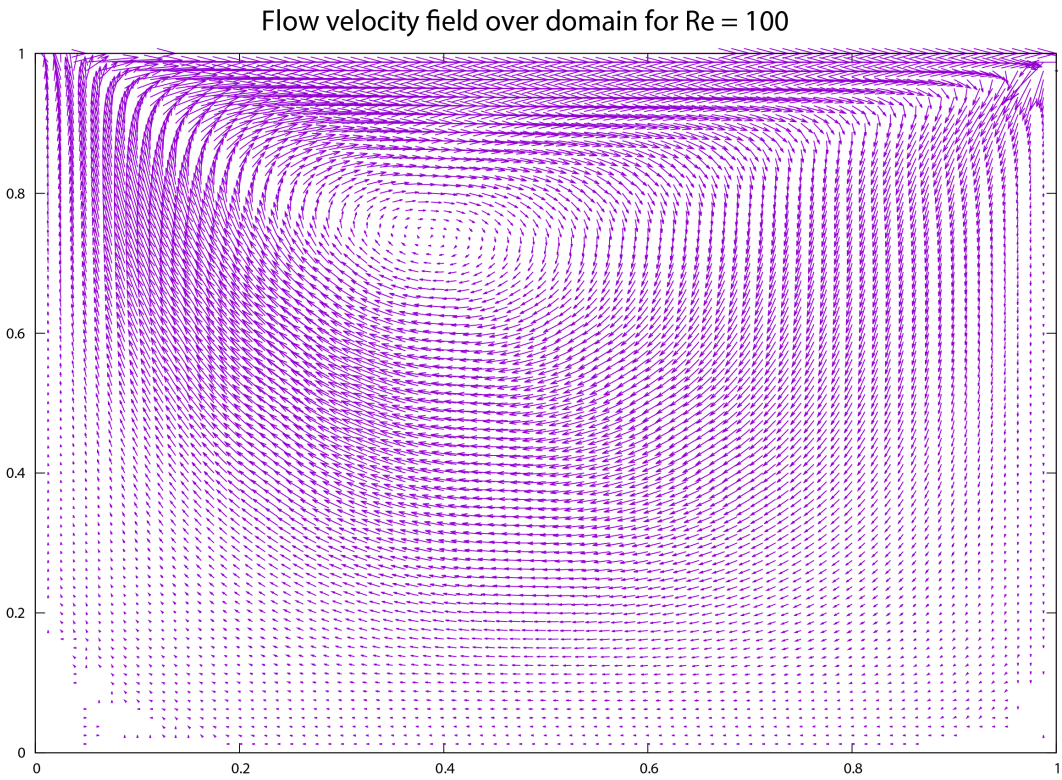


**Figure 12:** Diagram of the velocity vector field in the stationary state for the driven cavity example with $Re = 100$ in a grid of 6400 points (80x80).

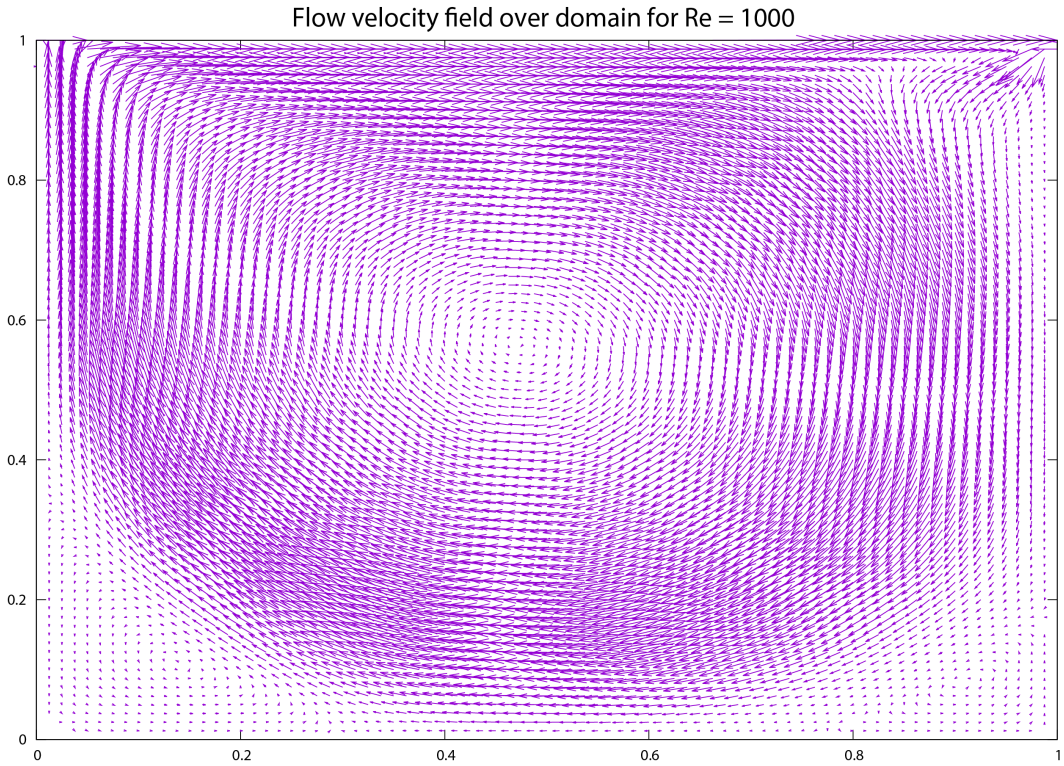


**Figure 13:** Diagram of the velocity vector field in the stationary state for the driven cavity example with $Re = 1000$ in a grid of 6400 points (80x80).

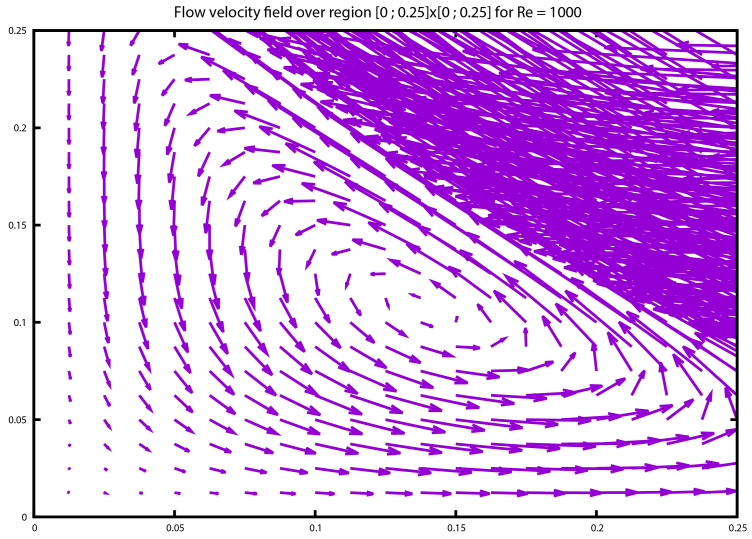


**Figure 14:** Diagram of the velocity vector field in the stationary state for the driven cavity example with $Re = 1000$ in a grid of 6400 points (80x80). Detail of the left lower corner with a secondary vortex, for region [0 ; 0.25]x[0 ; 0.25].

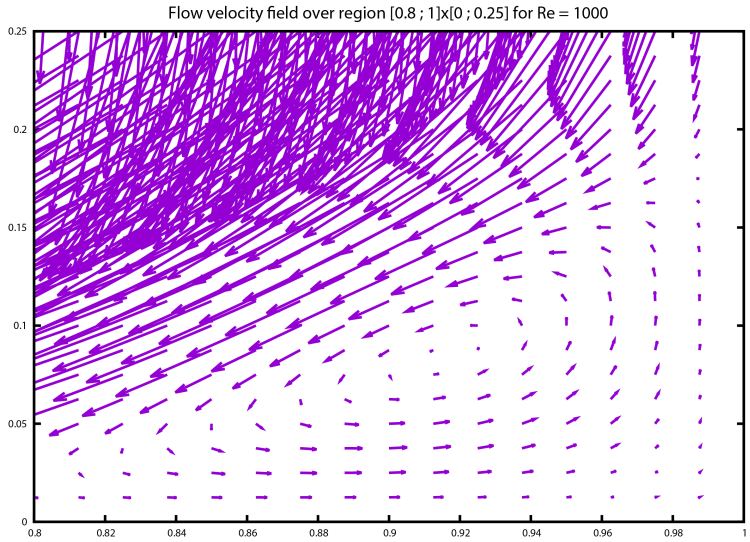


**Figure 15:** Diagram of the velocity vector field in the stationary state for the driven cavity example with $Re = 1000$ in a grid of 6400 points (80x80). Detail of the right lower corner with a secondary vortex, for region [0.8 ; 1]x[0 ; 0.25].

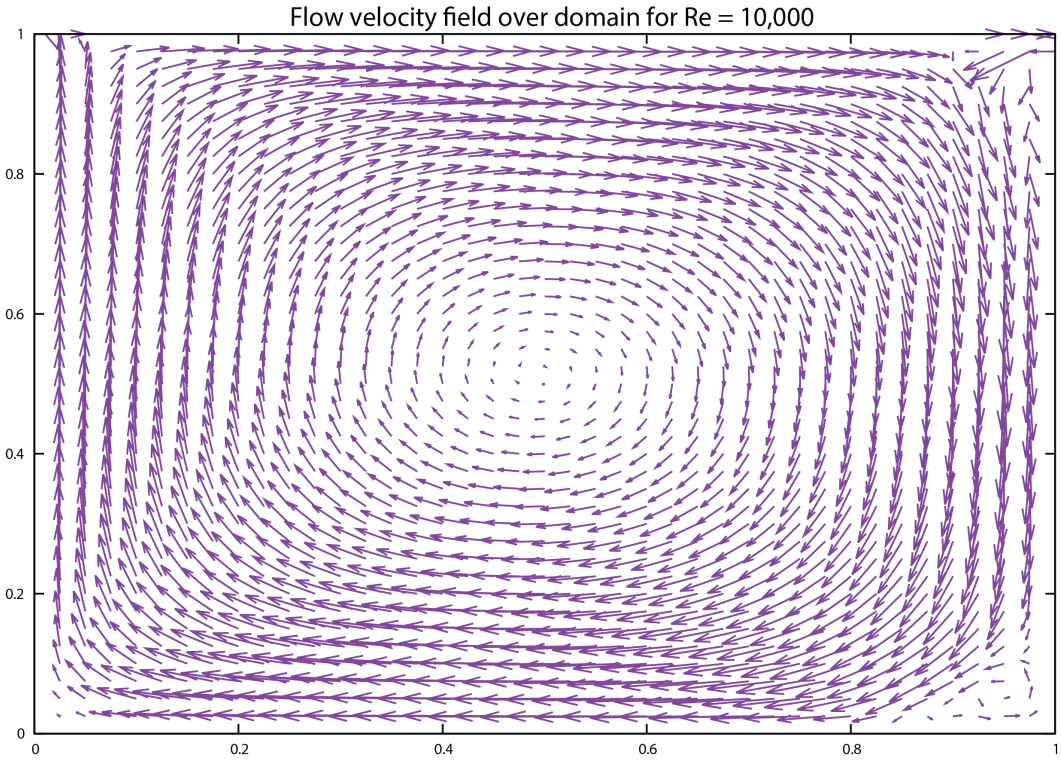


**Figure 16:** Diagram of the velocity vector field in the stationary state for the driven cavity example with $Re = 10,000$ in a grid of 1600 points (40x40).

# Appendix 2: Reference values for driven-cavity problem

| Position y | $Re = 100$ | $Re = 1000$ | $Re = 10,000$ |
|---|---|---|---|
| 1.0000 | 1.00000 | 1.00000 | 1.00000 |
| 0.9766 | 0.84123 | 0.65928 | 0.47221 |
| 0.9688 | 0.78871 | 0.57492 | 0.47783 |
| 0.9609 | 0.73722 | 0.51117 | 0.48070 |
| 0.9531 | 0.68717 | 0.46604 | 0.47804 |
| 0.8516 | 0.23151 | 0.33304 | 0.34635 |
| 0.7344 | 0.00332 | 0.18719 | 0.20673 |
| 0.6172 | -0.13641 | 0.05702 | 0.08344 |
| 0.5000 | -0.20581 | -0.06080 | -0.03111 |
| 0.4531 | -0.21090 | -0.10648 | -0.07540 |
| 0.2813 | -0.15662 | -0.27805 | -0.23186 |
| 0.1719 | -0.10150 | -0.38289 | -0.32709 |
| 0.1016 | -0.06434 | -0.29730 | -0.38000 |
| 0.0703 | -0.04775 | -0.22220 | -0.41657 |
| 0.0625 | -0.04192 | -0.20196 | -0.42537 |
| 0.0547 | -0.03717 | -0.18109 | -0.42735 |
| 0.0000 | 0.00000 | 0.00000 | 0.00000 |

**Table 3:** Reference values for $u$ velocity along vertical line through geometric center

| Position x | $Re = 100$ | $Re = 1000$ | $Re = 10,000$ |
|---|---|---|---|
| 1.0000 | 0.00000 | 0.00000 | 0.00000 |
| 0.9688 | -0.05906 | -0.21388 | -0.54302 |
| 0.9609 | -0.07391 | -0.27669 | -0.52987 |
| 0.9531 | -0.08864 | -0.33714 | -0.49099 |
| 0.9453 | -0.10313 | -0.39188 | -0.45861 |
| 0.9063 | -0.16914 | -0.51550 | -0.41496 |
| 0.8594 | -0.22445 | -0.42665 | -0.36737 |
| 0.8047 | -0.24533 | -0.31966 | -0.30719 |
| 0.5000 | 0.05454 | 0.02526 | 0.00831 |
| 0.2344 | 0.17527 | 0.32235 | 0.27224 |
| 0.2266 | 0.17507 | 0.33075 | 0.28003 |
| 0.1563 | 0.16077 | 0.37095 | 0.35070 |
| 0.0938 | 0.12317 | 0.32627 | 0.41487 |
| 0.0781 | 0.10890 | 0.30353 | 0.43124 |
| 0.0703 | 0.10091 | 0.29012 | 0.43733 |
| 0.0625 | 0.09233 | 0.27485 | 0.43983 |
| 0.0000 | 0.00000 | 0.00000 | 0.00000 |

**Table 4:** Reference values for $v$ velocity along horizontal line through geometric center